Strål
säkerhets
myndigheten
Swedish Radiation Safety Authority

Authors:
Michael J. Apted
Randy Arthur
David Bennett
David Savage
Göran Sällfors
Håkan Wennerström

Research

2010:31

Buffer erosion: An overview of concepts and potential safety consequences

Report number: 2010:31 ISSN: 2000-0456
Available at www.stralsakerhetsmyndigheten.se

Title: Buffer erosion: An overview of concepts and potential safety consequences
Report number: 2010:31
Author: : Michael J. Apted[1], Randy Arthur[1], David Bennett[2], David Savage[3], Göran Sällfors[4] and Håkan Wennerström[5]
1. INTERA Incorporated, 3900 s. Wadsworth Blvd., Suite 555, Denver, Colorado 80235, USA;
2. TerraSalus Limited, Orchard House, Church Lane, Bisbrooke, Oakham, Rutland LE15 9EL, UK;
3. Savage Earth Associates Limited, 32 St Alban's Avenue, Queen's Park, Bournemouth BH8 9EE, UK;
4. GeoForce AB, c/o Sällfors, Billdals Almväg 9, 42738 Billdal, Sweden;
5. Dept. of Chemistry, Physical Chemistry 1, Box 124, Lund University, 22100, Lund, Sweden.
Date: November 2010

This report concerns a study which has been conducted for the Swedish Radiation Safety Authority, SSM. The conclusions and viewpoints presented in the report are those of the author/authors and do not necessarily coincide with those of the SSM.

SSM Perspective

In its safety analysis SR-Can, SKB reported preliminary results and conclusions on the mechanisms of bentonite colloid formation and stability, with a rough estimate of the consequences of loss of bentonite buffer by erosion. With the review of SR-Can the authorities (SKI and SSI) commented that erosion of the buffer had the greatest safety significance, that the understanding of the mechanisms of buffer erosion was inadequate, and that more work would be required to arrive at robust estimates of the extent and impacts of buffer erosion. After the SR-Can report, SKB started a two-year research project on buffer erosion. The results from this two-year project have been reported in several SKB technical reports.
SSM started this project to build up its own competence in the related scientific areas by a preliminary evaluation of SKB's research results.

Background

The bentonite buffer is an important barrier in the KBS-3 repository concept for final disposal of spent nuclear fuel. Montmorillonite is the primary mineral component of bentonite. This clay mineral will form a stable solid or gel under environmental conditions that are expected to occur during most of the safety-related period of repository evolution at potential repository sites in Sweden. Should glacial meltwaters having an extremely low ionic strength penetrate into the repository depths during future glaciation periods, however, the montmorillonite could potentially be dispersed in the form of suspended colloidal particles that are transported away from deposition holes by groundwater flowing in fractures. This process is usually referred to as buffer (chemical) erosion.

Objectives of the project

The processes of buffer erosion are related to several scientific areas and an understanding of them needs a multidisciplinary approach. The aim of this project is to build up SSM's competence in the related areas and to prepare SSM for the coming review of SKB's safety report accompanying its license applications planned in 2011.

Results

This report provides an overview of surface-chemical, physical (including rheological) and geochemical processes that could be important in controlling erosional mass losses of the buffer in a KBS-3 repository for spent nuclear fuel. The type of erosion considered in this overview could result from the formation of clay colloids by contact of the bentonite buffer with dilute solutions, such as glacial meltwaters that could migrate to repository depths from a warm-based ice sheet. Theoretical concepts and experimental studies relevant to the advective and diffuse transport of colloidal clay gels and sols that could form as bentonite expands into a fracture intersecting a deposition hole are reviewed. Potential impacts on repository safety caused by the effects of buffer erosion are considered qualitatively. Technical issues that could benefit from additional research are also identified.

Project information

Project management: Jinsong Liu
Project references: SSM 2009/1453, 2009/1454, 2009/1455, 2009/1565

Contents

1. Introduction

The bentonite buffer in a KBS-3 repository for spent nuclear fuel may be susceptible to mass losses by erosion should the constituent clay minerals be suspended as colloids that are then transported away from deposition holes in flowing groundwater[1]. This type of erosion, referred to generally in the present report as "*buffer erosion*", could occur in various scenarios, including those involving the transient migration of glacial meltwaters to repository depths, because stable suspensions of clay colloids tend to form in aqueous solutions that are relatively dilute (*e.g.*, Miller and Marcos, 2007; Missana *et al.*, 2003).

Figure 1_1 illustrates key features of a conceptual model of buffer erosion (Birgersson *et al.*, 2009). The figure represents a vertical cross section through a portion of a KBS-3V deposition hole that is intersected by a horizontal fracture. Free swelling of bentonite from the deposition hole outward into the fracture is resisted by friction forces acting within the bentonite and at the rock interface. The maximum penetration distance is reached when these counteracting forces equilibrate. Bentonite density and swelling pressure then decrease rapidly with increasing distance in the fracture. The rheological properties of the bentonite change accordingly from those of a solid $\rightarrow$ gel $\rightarrow$ fluid (which may also include a semi-fluid phase) [2]. Fluid properties are identical to those of groundwater at the penetration front. Clay colloids form near this front, and are lost by diffusion into the flowing groundwater. Bentonite fluids (*i.e.*, dispersions of bentonite colloids in water, not solids or gels) may also be lost by advection. More bentonite then extrudes into the fracture from the deposition hole to restore equilibrium. The resultant mass loss of bentonite from the deposition hole results in a decrease in buffer density.

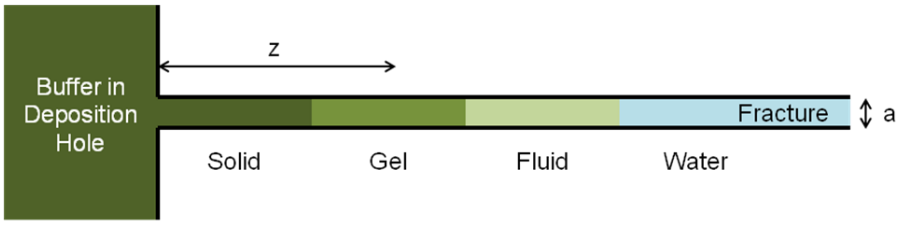

Figure 1_1. Conceptual model of buffer erosion. The swelling pressure of bentonite in the fracture decreases exponentially with increasing distance, *z*, and, at a given distance, with decreasing fracture aperture, *a* (Birgersson *et al.*, 2009). Models suggest that bentonite can extrude 11 m into a fracture having *a* = 1 mm if the groundwater flow velocity is about 1 m yr^{-1} (Neretnieks *et al.*, 2009). Penetration distances decrease with increasing groundwater flow velocities.

[1] This type of erosion differs from the release of bentonite particles at the buffer-groundwater interface by shear forces acting on the particles by rapidly flowing groundwater, or, in the process of "piping", by hydraulic forces acting on the buffer during saturation (Börgesson and Sandén, 2006; Liu and Neretnieks, 2006; Jusilla 2007). These latter types of erosion are not considered here.
[2] See Section 1.3 for notes regarding terminology.

Erosion could adversely impact safety functions of the buffer because the corresponding safety function indicators generally depend, either directly or indirectly, on the buffer's density. A case in point is illustrated in Figure 1_2, where swelling pressure (p_{swell}) measurements for an MX-80 bentonite are plotted as a function of dry density and molar NaCl concentrations in the coexisting aqueous solution[3]. The SR-Can safety assessment assumed that advective transport conditions in the buffer could be generated if $p_{swell} < 100$ kPa (SKB, 2006a). As can be seen in Figure 1_2, such low swelling pressures correspond to dry densities less than about 1000 kg m^{-3}. Börgesson and Hernelind (2006) determined that a loss of as little as 1200 kg of bentonite from a deposition hole, represented in their model by the complete loss of the half-circumference of two bentonite emplacement rings, would be sufficient to locally lower p_{swell} below the threshold value of 100 kPa. Although there is some uncertainty in this analysis regarding the assumed nature of friction forces acting between the buffer and rock, the results suggest that at higher mass losses adequate swelling pressure cannot be guaranteed and that advection in the buffer could therefore occur. This is a concern primarily because advection could increase the transport rate of corrodants to the canister's surface, thus potentially decreasing the containment lifetime of this engineered barrier. Buffer erosion was determined to be a key contributor to risk in SR-Can (SKB, 2006a).

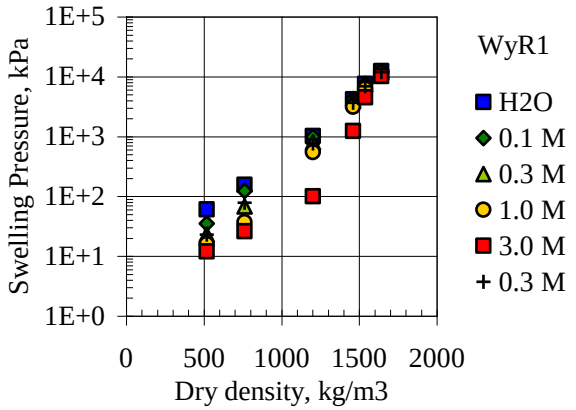

Figure 1_2. Plot showing variations in the swelling pressure of MX-80 bentonite as a function of dry density and aqueous NaCl concentration (SKB, 2006b; see also Karnland 1997). The montmorillonite component of the bentonite was in the Na-exchanged form.

Given the potential adverse impacts of buffer erosion on repository safety, The Swedish Radiation Safety Authority [Strålsäkerhetsmyndigheten (SSM)] commissioned the present report to help SSM prepare for the review of future license submittals from SKB for construction and operation of a KBS-3 repository at the Forsmark site.

[3] The initial dry density of the buffer in a KBS-3V repository will average about 1570 kg m^{-3} in order to achieve a target saturated density of 2000 ± 50 kg m^{-3} (SKB 2006a).

The objective of the report is to provide an overview of current understanding regarding features, events and processes governing buffer erosion and its potential impacts on repository safety.

The report is organized as follows. Previous models of buffer erosion and its treatment in SR-can are summarized below, together with notes on the terminology used in this report. Chemical and physical constraints on processes controlling buffer erosion are considered in Sections 2 and 3, respectively. Section 4 deals with interactions involving the buffer and groundwater. An evaluation of whether buffer mass losses by erosion could be minimized by the formation of filters composed of accessory minerals in bentonite is described in Section 5. Concluding remarks are summarized in Section 6, and Section 7 identifies issues for which additional research is recommended.

1.1 Historical background

Buffer erosion was first considered in the SR-Can Interim Process Report (SKB, 2004) (Figure 1.1_1). Erosion was assumed to occur only by diffusion of clay colloids into flowing groundwater (*i.e.*, advection of a bentonite fluid was not considered in this model). Conditions promoting the formation and stability of the colloids were accounted for using the concept of a critical coagulation concentration (CCC) for "free" (*i.e.*, uncomplexed) Ca^{2+}. Clay colloids were assumed not to form at the bentonite-groundwater interface if the Ca^{2+} concentration in the bentonite porewater was greater than the CCC. The CCC for Ca^{2+} was assumed to be 1 mM.

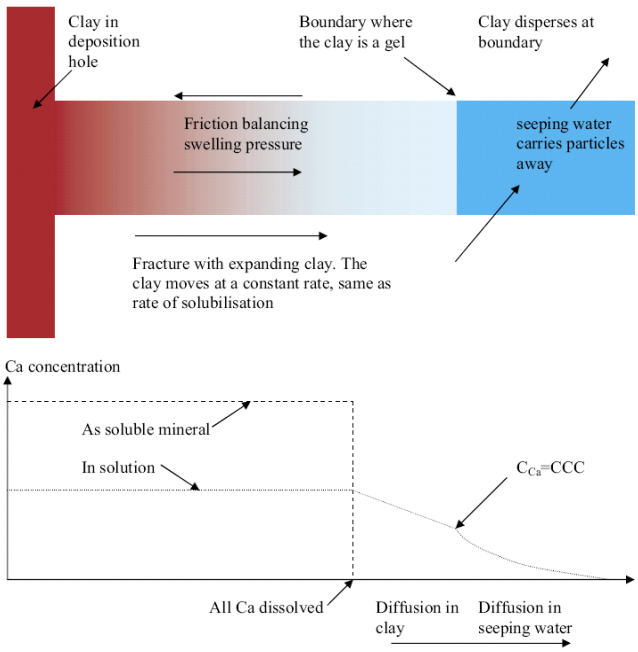

Figure 1.1_1. Conceptual model of buffer erosion (SKB, 2004). The buffer is assumed to extrude into a fracture under the control of swelling-pressure and friction forces. The concentration of Ca^{2+} in the seeping groundwater is less than the CCC. The Ca^{2+} concentration at the

interface between the groundwater and buffer is equal to the CCC (*i.e.*, because the gel is stable at that point). Calcium in the buffer porewater diffuses toward the groundwater, and this is accompanied by dissolution of calcite, a Ca-bearing mineral.

SKB assumed that at times in the future when the repository is overlain by a warm-based ice sheet, dilute glacial meltwaters having Ca^{2+} concentrations below the CCC could flow downward into the repository. A mass balance was used to estimate the extent to which the buffer would then be transformed into a stable colloidal suspension and carried away with the groundwater. This resulted in the following equation:

$$N_{day} = \left(\frac{Q_{eq}(c_i - c_w)}{\varepsilon_{day}(c_0 - c_i)} \right) \rho_{drydday}, \qquad (1.1\_1)$$

where N_{clay} refers to the mass of buffer lost per unit time (kg yr^{-1}), Q_{eq} stands for the equivalent flow rate (m^3 yr^{-1}), c_i represents the Ca^{2+} concentration in groundwater that has reacted with bentonite in the fracture ("leaving groundwater"; mol m^{-3}), c_w denotes the Ca^{2+} concentration in groundwater prior to reaction with bentonite in the fracture ("entering groundwater"; mol m^{-3}), c_0 refers to the concentration of Ca^{2+} that could be added to bentonite porewater by dissolution of soluble minerals (mol m^{-3}), ε_{clay} denotes buffer porosity, and $\rho_{dry,clay}$ stands for the dry density of the buffer. The equivalent flow rate was interpreted to represent the flow rate of groundwater that will carry away Ca^{2+} that diffuses into the groundwater from the buffer's porewater with an average concentration equal to the difference between c_i and c_w.

Equation (1.1_1) was evaluated under two limiting conditions regarding the amount of soluble calcite that was assumed to be initially present in bentonite: either 0 or 1 wt%. Any calcite in the buffer was assumed to dissolve completely and instantaneously. Other initial and boundary conditions included:

Q_{eq} = 0.001 m^3 yr^{-1},
c_0 = 10 mol m^{-3} (0 wt% calcite) or 1250 mol m^{-3} (1 wt% calcite),
c_i = CCC = 1 mmol m^{-3},
c_w = 0 mol m^{-3},
$\rho_{dry,clay}$ = 1600 kg m^{-3}, and
ε_{clay} = 0.4.

The results of the calculations indicated N_{clay} = 0.4 kg yr^{-1} for the first case (0 wt% calcite), and N_{clay} = 0.0032 kg yr^{-1} for the second case (1 wt% calcite). If it is assumed that buffer performance could be adversely affected if 1200 kg of bentonite erodes from the fracture/deposition hole (Börgesson and Hernelind, 2006), then these estimated erosion rates suggest that this could happen within about 3,000 to 375,000 years, depending on the amount of calcite initially present in the buffer.

Liu and Neretnieks (2006) used a revised version of the conceptual model discussed above to estimate buffer erosion rates. The revised model differed from the original model in two important respects. First, groundwater flow rates were modelled explicitly instead of using the equivalent flow rate (values for Q_{eq} were also calculated using groundwater flow parameters, however). Second, Liu and Neretnieks (2006) assumed that Ca concentrations in the buffer's porewaters were controlled by the solubility of trace amounts (0.7 wt.%) of gypsum rather than calcite. Gypsum was considered in this model because the solubility of calcite was considered to be too low to sustain Ca concentrations above the CCC. The concentration of Ca^{2+} buffered by gypsum solubility was assumed to be fixed at 9.8 mM.

Liu and Neretnieks (2006) used the FEMLAB computer program (Comsol, 2004) to solve for the integrated total flux of Ca along the extruded bentonite-groundwater boundary. The flux was then used to estimate the corresponding buffer erosion rate by assuming that the buffer was dispersed as a colloid and lost from the fracture and deposition hole if the concentration of Ca^{2+} in the buffer porewater fell below the CCC. Results using "central values" for groundwater flow parameters [hydraulic gradient (0.01), transmissivity (10^{-8} m^2 s^{-1}) and fracture aperture (10^{-4} m)] indicated that the erosion rate would be 0.11 kg yr^{-1}. This suggests that 1200 kg of bentonite would be lost in about 11,000 years, leading to the establishment of advective conditions thereafter.

An R&D program on buffer erosion was initiated by SKB in 2007. The status of this program was described in a series of workshop proceedings, SKB technical reports, and publications in scientific journals between 2007 and 2010. The results of this R&D program are considered in Sections 2 – 5 of the present report.

1.2 Treatment in SR-Can

The conceptual models described in Section 1.1 were not used to estimate buffer erosion rates in SR-Can. Rather, the rates were calculated using:

$$R_{buffer} = C_{Max} Q_{eq}, \qquad (1.2\_1)$$

where R_{buffer} stands for the erosion rate (kg yr^{-1}), C_{Max} refers to the maximum concentration of bentonite in a water suspension (50 kg m^{-3}) and Q_{eq} denotes the equivalent flow rate (m^3 yr^{-1}) (SKB, 2006a). Bentonite was assumed to consist of a pure Na-montmorillonite. The C_{max} value was selected by SKB based on unreferenced empirical observations.

Equation (1.2_1) was evaluated by assuming that groundwater flow rates at repository depth would be similar to those observed at the Forsmark and Laxemar sites today (SKB, 2006a). The corresponding Q_{eq} distributions were abstracted from results of three hydrogeological models: 1) a fully correlated discrete fracture network (DFN) model; 2) a semi-correlated DFN model, and 3) a continuous porous medium (CPM) model. The DFN models were

considered to be conservative because they tend to predict more severe consequences with respect to solute release and transport. Glacial meltwaters were assumed to migrate to repository depths over a 25,000 year interval within the 120,000 year reference glacial cycle. The models also considered possible spalling of the host rock near deposition holes. Spalling is a potential concern because it could increase the porosity and permeability of the host rock.

Results obtained using the semi-correlated DFN model for the Forsmark site without spalling indicated that 1200 kg of the buffer (*i.e.* the threshold value for initiation of advective transport) would be lost from about 3% of the deposition holes (SKB, 2006a). The alternative flow models predicted that buffer losses would be less than 1200 kg in all the deposition holes. With spalling, more than 1200 kg of the buffer was predicted to be lost after 25,000 years from 15% of the deposition holes using the fully correlated DFN model, from 35% of the holes using the semi-correlated DFN model, and from none of the holes using the CPM model. Similar estimates using the semi-correlated DFN model for the Laxemar site indicated that at least 1200 kg of bentonite would be lost from 40% of the deposition holes after 25,000 years.

These results suggest that advective conditions in the buffer could be generated in a substantial number of deposition holes over a reasonable range of hydrogeological conditions at the Forsmark and Laxemar sites. SKB noted, however, that the accuracy of erosion rates estimated using Equation (1.2_1) is highly uncertain because the calculation model was not built upon a mechanistic understanding of processes controlling colloid release from compacted buffer materials (SKB, 2006a). Repulsive forces acting to separate, and thus stabilize, colloidal suspensions were not considered in the model, for example, and these forces should act to increase the erosion rate. On the other hand, SKB noted that preliminary experimental and theoretical evidence (unreferenced) indicated that colloid release from commercial bentonites, especially those in which Ca^{2+} is an important exchangeable cation in montmorillonite, are much less susceptible to colloid formation than are montmorillonites in the pure Na form (SKB, 2006a). For these reasons, SKB concluded that it is possible that actual erosion rates for the buffer could be lower, or higher, than those estimated in SR-Can. The underlying reasons for this uncertainty are considered further in Sections 2 – 4 of the present report.

1.3 Terminology

The colloid nomenclature adopted here is largely that recommended by the International Union for Pure and Applied Chemistry (IUPAC) (see Everett, 1971). C*olloids* are solid particles (*e.g.*, clays) having a length between 1 nm and 1μm in at least one direction. A *colloidal dispersion* is a system in which the colloidal particles are dispersed in a continuous medium such as an aqueous solution.

The particles in a colloidal system may be discrete or may form continuous network structures having basic units that are in the range of colloidal dimensions. A *sol* is a fluid, or semi-fluid, colloidal system. A *gel* is a colloi-

dal system having a continuous network structure and a finite yield stress. *Repulsive gels* result from electroviscous effects that tend to inhibit colloid movement in systems having low aqueous salt concentrations and high colloid concentrations (Lagaly, 2006). *Attractive (or cohesive) gels* form in aqueous solutions having relatively high salt concentrations, which allow attractive forces between colloidal particles to outweigh repulsive forces. If the attractive forces become too strong the gel network disintegrates, forming *flocs*, which settle into a sediment.

The distinction between sols, gels and flocs is critical because it is generally believed that the buffer will not be susceptible to erosion unless sols form (*e.g.*, Neretnieks *et al.*, 2009). This is an important concept in the context of buffer erosion because stability relations among montmorillonite flocs, sols, attractive gels and repulsive gels can be related to environmental variables, such as electrolyte concentration and clay content (*e.g.*, Figure 1.3_1). These boundaries are somewhat problematic for *thixotropic gels*, which tend to maintain their shape until they are subjected to shearing or some other disturbance. *Percolation gels* are those for which the sol-gel transition in a colloidal system is defined based on structural rather than rheological changes. It is worth emphasizing here that montmorillonite sols tend to be stable in relatively dilute solutions having relatively low clay/water ratios. These constraints are considered further in Section 4.3.

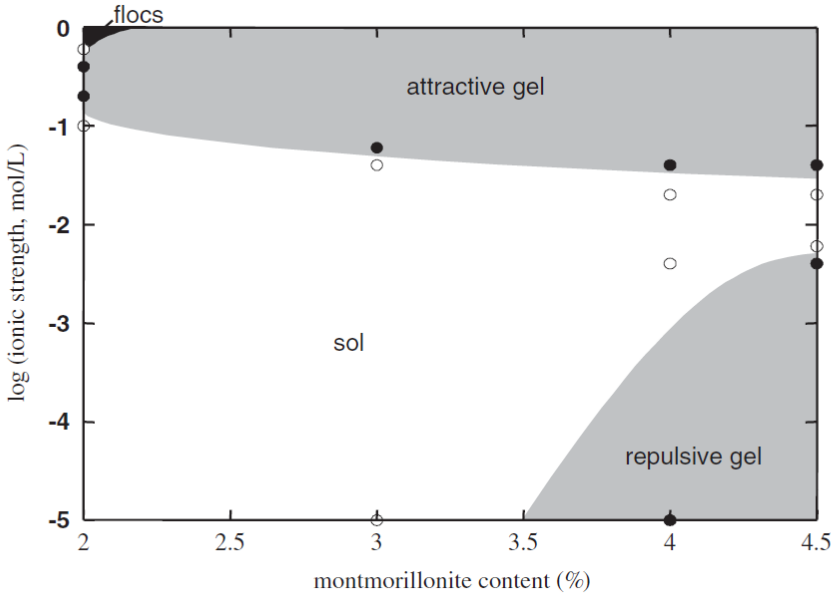

Figure 1.3_1. Sol-gel diagram for Na-montmorillonite in NaCl solutions (Abend and Lagaly, 2000). The stability fields of flocs, attractive gels, repulsive gels and sols are shown in relation to ionic strength and montmorillonite content. Symbols represent experimental observations indicating that gels (solid symbols) or sols/flocs (open symbols) are stable.

Birgersson *et al.* (2009) characterized bentonite gels and sols based on their rheological properties. Fluids consisting of bentonite sols have Newtonian

viscosities that are fixed and independent of shear rate. Semi-fluids consisting of bentonite sols tend to follow a non-linear, power-law relation between shear stress and shear rate, and viscosities tend to decrease with increasing shear rate in these non-Newtonian fluids. Gels behave like sedimentary clays. Their shearing behaviour is best described in terms of a shear resistance that must be overcome before further shearing can occur.

The rheological properties of bentonites depend strongly on the water ratio (w_r), given by

$$w_r = \frac{m_w}{m_s},$$

where m_w stands for the mass of water and m_s refers to the solid mass (*i.e.*, dry weight of bentonite). Bentonites containing only a pure Na-montmorillonite are (Birgersson *et al.*, 2009):

- a gel if $w_r < 35$;
- non-Newtonian fluid (*i.e.*, a semi-fluid) if w_r is between 35 and 100; and
- a Newtonian fluid if w_r is between 100 and 1000.

At $w_r > 1000$ the effects of montmorillonite content on the rheological properties of the fluid become negligible. Pure montmorillonite sols can therefore exist only if $w_r > 35$. The w_r values defining each of the above categories are somewhat lower for MX-80 bentonites (Birgersson *et al.*, 2009).

2. Chemical aspects of buffer erosion

This section considers chemical aspects of buffer erosion. Section 2.1 discusses various chemical constraints on the erosion rate. Section 2.2 discusses associated issues related to the formation and stability of clay colloids. Section 2.3 considers some relevant experimental work performed and recently reported by SKB and its contractors. Physical aspects of buffer erosion are considered in Section 3.

2.1 Chemical constraints on erosion rates

The models of buffer erosion described earlier (Section 1.1) assumed that clay particles would be swept away by water flowing in a fracture, but the actual mechanisms involved were not specified. Neretnieks *et al.* (2009) extended these models to account for forces that would control the expansion of bentonite from a deposition hole into a fracture (dynamic force-balance model), and for the effects of particle and ionic concentrations on the viscosity of the expanded bentonite (viscosity model). The force-balance and viscosity models were combined into an overall model of buffer erosion, which accounts for both the Brownian motion of individual clay colloids into the flowing groundwater and for the advection of sols that form within the fracture as the bentonite expands and becomes less dense and less viscous. Chemical aspects of the force-balance and viscosity models are considered in Sections 2.1.1, 2.1.2 and 2.1.3. An alternative modelling approach based on variations in the rheological properties of bentonite as a function of water content was developed by Birgersson *et al.* (2009) (see Section 3).

Before proceeding to the discussions below, it is worthwhile reviewing results obtained using the buffer erosion model described by Neretnieks *et al.* (2009). Moreno *et al.* (2008; 2009) evaluated this model for the idealized case of two-dimensional groundwater flow in a horizontal fracture intersecting a deposition hole in a KBS-3V repository. The fracture aperture was assumed to be 1 mm. Bentonite was assumed to consist of pure Na-montmorillonite and the groundwater was represented by a dilute NaCl solution. This simplified system was assumed to be conservative because Ca-dominated clays do not swell as much as their Na-dominated counterparts and are less susceptible to colloid formation (Neretnieks *et al.*, 2009). The Darcy flow equation, solute diffusion equations, and governing equations underpinning the force-balance and viscosity models were evaluated simultaneously using a numerical approach and solver (Comsol Multiphysics 2009). As noted above, the force-balance and viscosity models account explicitly for the effects of colloid and ion concentrations on the expansion of bentonite within the fracture and on resultant changes in viscosity.

Model results are summarized in Table 2.1_1 (Neretnieks *et al.*, 2009). As can be seen, the erosion rate increases, and the length of the fracture penetrated by bentonite decreases, with increasing groundwater velocity. The

erosion rate is proportional to the water velocity raised to the power 0.41 (Neretnieks *et al.*, 2009). The rate is also directly proportional to the fracture aperture. Note that the erosion rate and fracture penetration distance for the two lowest water velocities were extrapolated by Moreno *et al.* (2009) from model results for the four higher water velocities. This is because the numerical method became unstable when the velocity was less than about 0.95 m yr^{-1}. Neretnieks *et al.* (2009) note that these results are preliminary and that the erosion rate for a given water velocity could be higher or lower than the values given in Table 2.1_1. This is because the effects of ion transport on the viscosity have not been adequately accounted for in systems containing both Na^{+} and Ca^{2+} ions.

Table 2.1_1. Erosion rates and corresponding penetration distances of bentonite in fractures as calculated by Moreno *et al.* (2009) using the buffer erosion model (Neretnieks *et al.*, 2009).

Water velocity (m yr^{-1})	*Erosion rate (g yr^{-1})*	*Penetration distance (m)*
0.10	11	34.6
0.32	16	18.5
0.95	26	11.5
3.15	43	7.0
31.50	117	2.1
315.00	292	0.5

2.1.1 Force-balance model

The expansion of the buffer from a deposition hole into an intersecting fracture will be controlled by a number of forces acting on the individual clay particles in bentonite. Neretnieks *et al.* (2009) developed a dynamic force-balance model of the expansion process. The model accounts for the gravity and buoyant force (F_g), forces resulting from changes in the chemical potential in a concentration gradient (diffusional force; F_μ), van der Waals attractive forces between clay particles (F_{vdW}), repulsive forces between the particles resulting from charges within and on the surfaces of the particles (diffuse double layer forces, F_{DDL}), and friction forces (F_η) acting on the particles as they move through the aqueous phase as a result of imbalances among the other forces. Because changes in particle velocity are expected to be slow as the buffer expands into a fracture, acceleration can be neglected and the sum of the forces noted above must then always be equal to zero.

Chemical aspects of the force-balance model are mainly incorporated in the attractive van der Waals and repulsive double-layer forces between individual clay particles. These forces are considered further in Section 2.1.3. Expressions for F_g, F_μ and $F_{\eta.}$ are described by Liu *et al.* (2009) and Neretnieks *et al.* (2009). Liu *et al.* (2009) evaluated the force-balance model using magnetic resonance imaging (MRI) data characterizing the vertical expansion of a Na-montmorillonite pellet in a test tube filled with distilled water. Agreement between the MRI data and model predictions was good during the latter stages of expansion (*i.e.*, after about 20 hours), but not initially. The dis-

agreement was attributed by Liu *et al.* (2009) to heterogeneous wetting of the initially dry pellet.

2.1.2 Viscosity model

Expansion of bentonite from a deposition hole into a fracture will result in changes in the bentonite density as a function of distance in the fracture. The density will vary from that of the buffer at the fracture/deposition hole interface to a value approaching the density of water at the point of maximum extension of the bentonite in the fracture. The changes in density will result in corresponding changes in the volume fraction, ϕ, of clay particles in the expanded bentonite. The changes in ϕ will in turn affect the viscosity. The expanded bentonite may flow as a fluid or semi-fluid phase when ϕ reaches a threshold value marking the transition from a gel to a sol.

The force-balance approach described in Section 2.1.1 (see also Section 2.1.3) can be used to predict changes in the density (and ϕ) of bentonite extruded into a fracture from a deposition hole. A complementary viscosity model was developed by Moreno *et al.* (2009) (see also Neretnieks *et al.*, 2009) to relate changes in ϕ to corresponding changes in the viscosity of bentonite gels/sols. Advective transport of the sols, along with the groundwater flowing in the fracture, can then be accounted for using the buffer erosion model (Neretnieks *et al.*, 2009).

The viscosity model is based on the concept of a co-volume of a colloidal particle. The co-volume is defined as the volume over which a given particle can rotate freely without touching other particles in a colloidal suspension. It is determined both by the physical size of the particle as well as by interactions involving the particle's electrical double layer and those of its nearest neighbours (see Section 2.1.3). The co-volume thus depends on the physical volume fraction (*i.e.*, ϕ) and on properties of the colloidal suspension, such as the ionic composition of the aqueous phase, that control the effective thickness of the electrical double layer.

The co-volume fraction of a clay particle is given in the viscosity model by (Neretnieks *et al.*, 2009):

$$\phi_{cov}^{\kappa} = \frac{V_{cov}}{V_p}\phi = \frac{2}{3}\frac{(l_s + 2m\kappa^{-1})^3}{l_s^2\delta_s n}\phi, \qquad (2.1.2\_1)$$

where V_{cov} stands for the co-volume of a colloidal particle, which is assumed to consist of stacks of individual clay sheets, V_p refers to the physical volume of the particle, l_s represents the lateral extent of the sheets, κ^{-1} denotes the double-layer thickness (see Section 2.1.3), m is an adjustable parameter representing a multiple of this thickness, δ_s refers to the sheet thickness and n represents the number of sheets in a stack. An empirical expression relating the co-volume fraction of clay particles to the relative viscosity of a gel/sol is given by (Neretnieks *et al.*, 2009):

$$\frac{\eta}{\eta_w} = 1 + a\phi_{cov}^{\kappa} + b(\phi_{cov}^{\kappa})^2 + c(\phi_{cov}^{\kappa})^3, \qquad (2.1.2\_2)$$

where η refers to the viscosity of the suspension, η_w denotes the viscosity of water and a, b, and c are coefficients. Neretnieks *et al.* (2009) regressed Equation (2.1.2_2) using experimental data on relative viscosities and ϕ determined in clay colloidal systems over a range of different ionic strengths. The regression was found to be optimized when it assumed that l_s = 220 nm and m = 1, giving:

$$\frac{\eta}{\eta_w} = 1 + 1.022\phi_{cov}^{\kappa} + 1.358(\phi_{cov}^{\kappa})^3. \qquad (2.1.2\_3)$$

This empirical expression was used in the viscosity model to calculate the viscosity of bentonite gels and sols. The calculated values depend on the volume fraction of the colloidal particles in the gel/sol and on the ionic composition of the aqueous phase. Given the empirical nature of Equation (2.1.2_3), it is not clear whether the viscosity model is appropriate for conditions that lie outside the range of clay compositions and solution compositions considered in the experimental dataset upon which the equation is based.

2.1.3 DLVO theory

Terms for the van der Waals force and diffuse double layer force in the force-balance model (Section 2.1.1) were derived by Liu *et al.* (2009) and Neretnieks *et al.* (2009) based on DLVO theory. Given its central importance to the overall force-balance modelling approach, this theory is described in further detail here. Perceived limitations in the theory are summarized in Section 2.1.4. Section 2.2 considers applications of DLVO theory in interpretations of the formation and stability of clay colloids.

2.1.3.1 Electrical conditions at the clay-water interface

DLVO is an acronym derived from the surnames of researchers that developed this theory of colloid stability (Derjaguin and Landau, 1941; Verwey and Overbeek, 1948). The theory is based on electrical properties of the colloid-water interfacial region and on interaction energies that come into play when two charged colloidal particles approach one another. Kruyt (1952), Adamson (1967), van Olphen (1977), Sposito (1984), Stumm and Morgan (1996) and Evans and Wennerström (1999) provide detailed descriptions of the DLVO model and its application to idealized systems and clay-water systems.

The electrostatic forces considered in the DLVO conceptual model arise from electrical interactions at the solid-liquid interface (Figure 2.1.3.1_1).

For clay colloids a net electrical charge on the particles arises from several sources that can be represented by (Stumm and Morgan, 1996):

$$\sigma_p = \sigma_o + \sigma_H + \sigma_{is} + \sigma_{os} \qquad (2.1.3.1\_1)$$

where σ_p stands for the net particle charge, σ_o denotes the permanent structural charge resulting from isomorphous substitutions on tetrahedral and octahedral sites in the clay's crystalline lattice, σ_H refers to the net proton charge resulting from proton-exchange reactions involving ionizable surface hydroxyl groups (represented by S-OH, where S includes Si, Al, *etc.*), σ_{is} stands for an inner-sphere complex charge and σ_{os} represents an outer-sphere complex charge (all charges have units of C m^{-2}). The latter two charges represent contributions to the net particle charge resulting from the specific adsorption of cations and anions by surface hydroxyl groups.

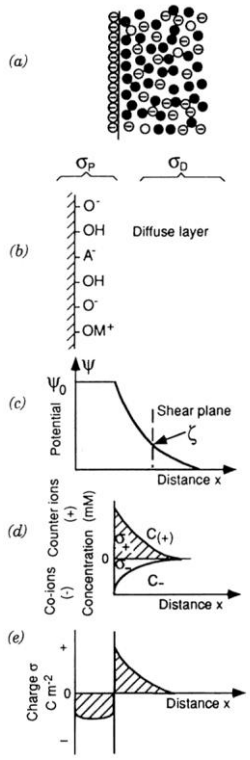

Figure 2.1.3.1_1. The diffuse double layer (after Stumm and Morgan, 1996). The diffuseness of the double layer results from thermal motions in the aqueous phase (*a*). Binding of H^+, O^{2-}, cations (M^{2+}) and anions (A^-) can occur on surface sites at the solid-water interface (*b*). The electrical potential (ψ) decreases with increasing distance outward into the diffuse layer from the surface, where the potential is ψ_0 (*c*). The zeta potential (ζ) is the potential at the shear plane of a moving particle. Variations in the charge distribution of cations and anions are shown in (*d*), and (*e*) shows the corresponding net excess charge.

The existence of charged colloidal particles in an aqueous electrolyte solution creates an electrical double layer of charge (Figure 2.1.3.1_1a, b). One layer corresponds to charges on the particle's surface, as discussed above, and the other is a compensating net charge that is spread out in a diffuse layer extending outward into the aqueous phase. Electrical neutrality in this interfacial region requires that

$$\sigma_p + \sigma_d = 0, \qquad (2.1.3.1\_2)$$

where σ_d refers to the total net charge in the diffuse layer.

The Gouy-Chapman model of the electrical double layer (*e.g.*, Adamson, 1967) establishes a simple relation between particle charge and electrical potential at the particle's surface. This model assumes that the particle's surface is a uniform infinite plane of charge and that aqueous ions exist as point charges in a uniform medium characterized by the dielectric constant. For a charge-symmetric electrolyte under such conditions, the relation between surface charge and surface potential (ψ_o; in V) is given by (*e.g.*, Stumm and Morgan, 1996):

$$\sigma_p = (8\varepsilon\varepsilon_o n_s k_B T)^{1/2} \sinh\left(\frac{ze\psi_o}{2k_B T}\right), \qquad (2.1.3.1\_3)$$

where ε denotes the relative dielectric constant of water (78.5 at 25°C), ε_o represents the electric permittivity of free space (8.854 x 10^{-12} C V^{-1} m^{-1}), n_s stands for the number concentration of ion pairs (cm^{-3}), k_B refers to the Boltzmann constant (1.3805 x 10^{-23} J K^{-1}), T denotes temperature (K), z represents ionic valence, and e stands for the elementary charge (1.60219 x 10^{-19} C). At 25°C, Equation (2.1.3.1_3) becomes:

$$\sigma_p = 0.1174 c_s^{1/2} \sinh\left(\frac{ze\psi_o}{2k_B T}\right) \qquad (2.1.3.1\_4)$$

where c_s refers to electrolyte concentration (M). Note that if ψ_o << 25 mV at 25°C,

$$\sigma_p = 2.5 I^{1/2} \psi_o \qquad (2.1.3.1\_5)$$

where I refers to ionic strength (see below) (M).

The potential decreases with increasing distance, *x*, outward from the surface into the diffuse layer. The potential at any point in the diffuse layer can be calculated using:

$$\frac{d^2\psi}{dx^2} = \frac{\kappa^2 \sinh\left(\frac{ze\psi}{k_B T}\right)}{\left(\frac{ze}{k_B T}\right)}, \qquad (2.1.3.1\_6)$$

where κ represents the reciprocal thickness of the double layer given by:

$$\kappa = \left(\frac{e^2 \sum_i n_i z_i^2}{\varepsilon \varepsilon_o k_B T} \right)^{1/2}, \qquad (2.1.3.1\_7)$$

and where n_i stands for the number concentration (cm^{-3}) of ions with valence z_i. A simplified version of Equation (2.1.3.1_6) that is valid when ψ << 25 mV is given by:

$$\frac{d^2\psi}{dx^2} = \kappa^2 \psi, \qquad (2.1.3.1\_8)$$

in which case,

$$\psi = \psi_o e^{(-\kappa x)} \qquad (2.1.3.1\_9)$$

and the potential thus decays exponentially at a rate that increases with decreasing thickness of the double layer (*i.e.*, with increasing values of κ).

Once the spatial distribution of electrical potentials in the diffuse layer is known, corresponding ionic concentrations can be calculated using the Boltzmann equation for cations and anions (*e.g.*, Adamson, 1967):

$$n_+ = n_o e^{(-ze\psi/k_B T)}, \text{ and} \qquad (2.1.3.1\_10)$$

$$n_- = n_o e^{(ze\psi/k_B T)}, \qquad (2.1.3.1\_11)$$

where n_+ and n_- represent local concentrations (mol cm^{-3}) of cations and anions in the diffuse layer, respectively, and n_o stands for ion concentrations in the bulk solution (*i.e.*, where $n_+ = n_-$ in accordance with charge-balance constraints). These local concentrations are important because, as discussed in the following section, they affect repulsive forces resulting from the interactions of double layers when two colloidal particles approach one another.

2.1.3.2 Interaction energies among colloidal particles

DLVO theory assumes that the stability of an aqueous colloidal system is controlled by a balance between electrostatic forces, which tend to repel particles of like charge, and attractive forces arising from van der Waals interactions. The concept is illustrated in Figure 2.1.3.2_1, which depicts changes in the total interaction energy, V_T, as two colloidal particles approach one another due to thermally driven Brownian motion. The net interaction energy, V_T, represents the sum of electrostatic double-layer repulsion (V_R) and van der Waals attraction (V_A) energies,

$$V_T = V_R + V_A. \qquad (2.1.3.2\_1)$$

At very small inter-particle distances, an additional repulsive force, indicated by the dotted line in Figure 2.1.3.2_1, arises due to the interaction of atomic electronic clouds (Born repulsion). Colloids are stable when $V_T > 0$ and unstable when $V_T < 0$.

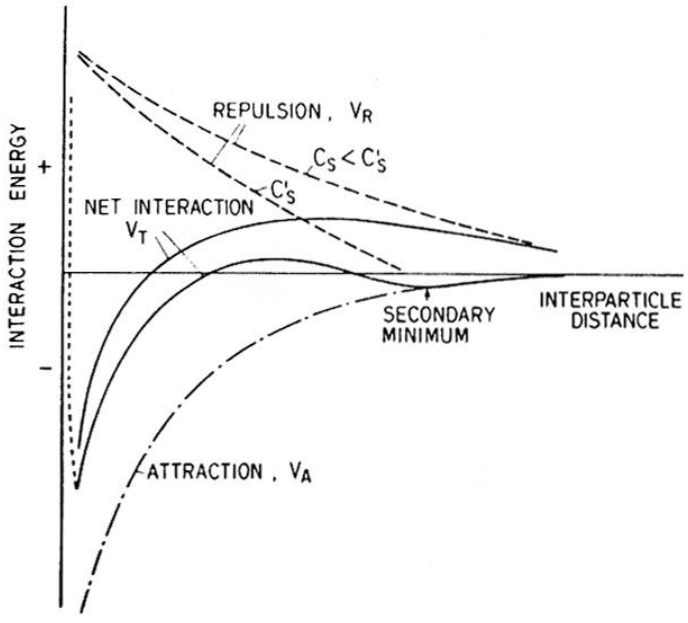

Figure 2.1.3.2_1. Schematic diagram illustrating the relation between interaction energies and separation distances between colloidal particles (Stumm and Morgan, 1996).

2.1.3.3 Colloids as parallel flat plates

Exact solutions to Equation (2.1.3.2_1) can be obtained for idealized systems in which colloidal particles exist as parallel flat plates or sheets. Argillaceous materials containing roughly parallel layers of clay minerals separated by an interlayer region containing variable amounts of an electrolyte solution closely approximate such systems.

Kruyt (1952) derived a solution for the repulsive term in Equation (2.1.3.2_1) for such systems (Figure 2.1.3.3_1). The total force acting on the plates was assumed to consist of an osmotic pressure force and a force arising from the electrical field. The latter force equals zero at the mid-plane (m) between the plates (*i.e.*, at $x = d/2$ in Figure 2.1.3.3_1) because $\mathrm{d}\psi/\mathrm{d}x = 0$ at that location. The total force is thus given by the osmotic pressure at the mid-plane position.

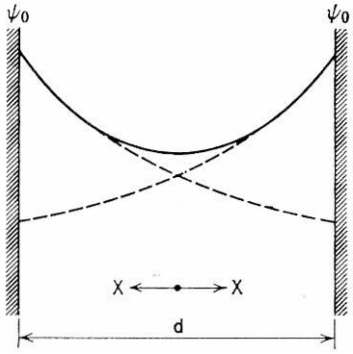

Figure 2.1.3.3_1. Interacting double layers between the surfaces of two colloidal particles represented by parallel flat sheets (Adamson, 1967). Potentials in the double layer adjacent to each sheet are shown as a function of distance from the surface, d, by the dashed lines. The solid line represents the total potential resulting from the interacting double layers.

The osmotic pressure, Δp, is given by (Kruyt, 1952):

$$\Delta p = p_m - p_o = n_{excess} k_B T = \left[n_o \left(e^{\frac{ze\psi_m}{k_B T}} + e^{\frac{-ze\psi_m}{k_B T}} \right) - 2n_o \right] k_B T \qquad (2.1.3.3\_1)$$

where p_m and p_o refer to pressures at the mid-plane and in the bulk aqueous phase, respectively, and n_{excess} stands for the excess concentration of cations and anions at m relative to their concentrations in the bulk solution. The expression on the right-hand side of the second identity in Equation (2.1.3.3_1) is obtained using Equations (2.1.3.1_10) and (2.1.3.1_11), and ψ_m refers to

the mid-plane potential. Rearrangement of Equation (2.1.3.3_1) yields (Kruyt, 1952):

$$\Delta p = 2n_o k_B T[\cosh(ze\psi_m / k_B T) - 1]. \qquad (2.1.3.3\_2)$$

This osmotic pressure represents the force per unit area causing colloidal particles to separate as a consequence of interactions involving their electrical double layers. Equation (2.1.3.3_2) represents the diffusive double layer force in the force-balance model developed by Neretnieks *et al.* (2009).

Integration of Equation (2.1.3.3_2) to obtain the total repulsive energy, V_R, in Equation (2.1.3.2_1) can be difficult because ψ generally varies as a complex function of distance between the colloidal particles. Kruyt (1952) noted, however, that for the case of relatively weak interactions between the particles (*e.g.*, when $\psi_m << 1$ V), the following relation can be used:

$$\frac{ze\psi_m}{k_B T} = 8\gamma e^{-\kappa m}, \qquad (2.1.3.3\_3)$$

where,

$$\gamma = \frac{(e^{\frac{ze\psi_o}{k_B T}} - 1)}{(e^{\frac{ze\psi_o}{k_B T}} + 1)}, \qquad (2.1.3.3\_4)$$

and where $m = d/2$, with d representing the separation distance between the particles as shown in Figure 2.1.3.3_1.

Equation (2.1.3.3_3) can be used in a first approximation[4] to Equation (2.1.3.3_2) to obtain:

$$\Delta p = n_o k_B T(8\gamma e^{-\kappa m})^2, \qquad (2.1.3.3\_5)$$

which can then be integrated from $x = \infty$ (bulk solution) to $x = m$ to yield (Kruyt 1952):

$$V_R = -2\int_{x=\infty}^{x=m} \Delta p dx = \frac{64 n_o k_B T}{\kappa}\gamma^2 e^{-2\kappa m}. \qquad (2.1.3.3\_6)$$

[4] Note that $\cosh(x) \approx 1 + x^2/2$ when x is small.

Equation (2.1.3.3_6) gives the total repulsive energy per unit area between colloidal particles for an idealized case in which the particles are represented by parallel flat plates.

DLVO theory attributes the attractive term, V_A, in Equation (2.1.3.2_1) to van-der Waals-London dispersion forces. These forces can be calculated in principle using Lifshitz theory (Lifshitz, 1956), which accounts for the macroscopic electrodynamic properties of the interacting media. In practice, however, relatively simple expressions for V_A are usually derived using an alternative approach developed by Hamaker (1937). In this approach the attraction energy between two bodies is calculated as the sum of London dispersion interactions among all pairs of atoms in the two bodies. The approach is valid as long as separations between the bodies do not approach atomic dimensions.

Using Hamaker's approach, V_A for two colloidal particles represented by parallel flat sheets can be calculated using (*e.g.*, Kruyt, 1952):

$$V_A = -\frac{A}{48\pi m^2}, \qquad (2.1.3.3\_7)$$

where *A* denotes the Hamaker constant (J) and *m*, as noted earlier, stands for the mid-plane position[5]. Values for the Hamaker constant are difficult to determine experimentally. For clay colloids, $A \approx 10^{-20}$ J appears to be a reasonable first approximation (*e.g.*, Lyklema, 1991; Swanton, 1995; Helmy, 1998).

Substituting Equations (2.1.3.3_6) and (2.1.3.3_7) into Equation (2.1.3.2_1) results in:

$$V_T = \frac{64 n_o k_B T}{\kappa} \gamma^2 e^{-2\kappa m} - \frac{A}{48\pi m^2}, \qquad (2.1.3.3\_8)$$

which gives the net total interaction energy between sheet-like colloidal particles as they approach one another. As is illustrated schematically in Figure 2.1.3.2_1, the net interactions are repulsive at relatively large particle separations, but become attractive when the particles reach a threshold separation that depends on the aqueous electrolyte concentration. The relation between this threshold distance and the critical coagulation concentration (CCC) of aqueous ionic species is considered further in the following section.

[5] A slightly more complicated form of Equation (2.1.3.3_7), which takes into account the thickness of individual clay particles, is used in SKB's force-balance model (Neretnieks et al., 2009). See also Section 2.2.3.

2.1.3.4 Effects of aqueous chemistry on colloid stability

The effects of electrolyte concentration on colloid stability are illustrated in Figure 2.1.3.2_1 by the two dashed curves showing variations in V_R as a function of inter-particle distance, and corresponding solid curves for V_T, the total interaction energy. Electrolyte concentration C_s is assumed to be smaller than C^*_s, and the diagram therefore indicates that colloidal suspensions (of planar geometry) are stable (*i.e.*, $V_T > 0$) over a broader range of inter-particle distances as the aqueous medium becomes more and more dilute. The secondary minimum in V_T when the electrolyte concentration equals C^*_s results in the formation of an attractive gel, which may re-disperse as a sol by stirring.

Separation distances among the particles in an aqueous colloidal suspension depend on the ionic strength of the medium because this parameter determines the rate at which the electrical potential decays with increasing distance outward from the surface into the double layer[6]. As noted in Section 2.1.3.1, the thickness of the double layer is generally taken as being equal to the reciprocal of the (Debye) parameter, κ, which is recast here as:

$$\kappa = \left(\frac{2F^2 I \, \mathrm{x} 10^3}{\varepsilon \varepsilon_0 RT} \right)^{1/2}, \qquad (2.1.3.4\_1)$$

where F refers to the Faraday constant, I represents ionic strength, given by

$$I = 1/2 \sum_i z_i^2 c_i, \qquad (2.1.3.4\_2)$$

and R stands for the gas constant and c_i stands for molar concentration. This equation indicates that the thickness of the double layer decreases as ionic strength increases, and this allows the individual particles in a colloidal suspension to move closer together. The particles will eventually form an attractive gel or floc if the double-layer thickness falls below a value corresponding to a threshold separation distance at which V_T first becomes negative. Conversely, stable colloids may form from a gel or floc if the ionic strength decreases to a point where V_T becomes positive. Chemical erosion of the buffer is thus more likely in situations where the buffer comes into contact with groundwaters that are relatively dilute.

The concept of a critical coagulation concentration (CCC), discussed in Section 1.1 can be related to compositional constraints on the aqueous phase that come into play when the threshold separation distance between colloidal particles is reached (*i.e.*, when $V_T = 0$). Considering the idealized case of

[6] Van der Waals interactions are not affected by ionic strength.

colloids as parallel flat plates, for example, Equation (2.1.3.3_8) indicates that under such conditions

$$\frac{64 n_o k_B T}{\kappa} \gamma^2 e^{-2\kappa m} = \frac{\mathrm{A}}{48\pi m^2} . \qquad (2.1.3.4\_3)$$

Kruyt (1952) rearranged this equation to give at 25°C

$$c = 8 \times 10^{-22} \frac{\gamma^4}{A^2 z^6}, \qquad (2.1.3.4\_4)$$

where c represents electrolyte concentration (mM) and where it is assumed that surface potentials in the expression for γ (Equation 2.1.3.3_4) are sufficiently high that $\gamma \approx 1$ and is independent of valency. The electrolyte concentration, c, is taken to be a critical coagulation concentration at, and below, which attractive forces between colloidal particles dominate, leading to the formation of attractive gels or flocs.

Equation (2.1.3.4_4) indicates that the CCC should vary according to an inverse 6-th power dependence on electrolyte valence, which is in reasonably good agreement with many empirical observations and is known as the rule of Schulze and Hardy (*e.g.*, Stumm and Morgan, 1996). When extended to systems in which the surface potential is low and $\gamma \neq 1$, the Schulze-Hardy rule invokes a $(1/z)^2$ dependence on valence (Kruyt, 1952). In either case, for negatively charged colloids such as clays, the CCC for cations tends to decrease strongly in the order monovalent > divalent > trivalent. Thus, although monovalent cations such as Na^+ or K^+ tend to be more abundant in natural waters than divalent cations, such as Ca^{2+} or Mg^{2+}, the latter type of cations are expected to more strongly influence colloid stability than the former type in accordance with the Schulze-Hardy rule. It is important to emphasize, however, that this rule applies only to supporting electrolytes that are "indifferent" in the sense that they do not react with other ions in the double layer and are not specifically adsorbed at the colloid's surface. Trivalent cations, such as Al^{3+} and Fe^{3+}, generally have very low concentrations in natural waters due to solubility constraints and because of hydrolysis and other complexation reactions, and may not behave like indifferent electrolytes with respect to clay minerals.

2.1.4 Limitations in DLVO theory

There is a general consensus that the conceptual basis of DLVO theory is substantially correct, but that the theory is also deficient in some important respects (*e.g.*, Kruyt, 1952; Swanton, 1995; Stumm and Morgan, 1996; Missana and Adell, 2000; Boström *et al.*, 2001; McBride and Baveye, 2002). Support for this view comes from studies involving direct force-balance measurements (see Iraelachvili and Adams, 1978; Israelachvili, 1991) of

adhesive and repulsive interactions among colloidal particles (see Swanton, 1995). These studies suggest that the treatment of van der Waals interactions in the DLVO model is generally valid as long as separation distances between colloidal particles are greater than atomic dimensions. The treatment of electrical double-layer interactions (Section 2.1.3) also appears to be valid, although important discrepancies between model predictions and experimental observations have been noted in some systems, especially those with divalent electrolytes (*e.g.*, see Section 2.1.4.1).

Limitations in DLVO theory arise for two general reasons: 1) oversimplification of the properties of real colloids, and 2) omission of "non-DLVO" forces that can be important under certain circumstances. These limitations can be categorized as follows (Swanton, 1995):

- The theory treats colloidal particles as if they were smooth bodies having ideal geometries. Real colloids are irregular in size and shape, however, and have rough surfaces. Surface roughness can affect both the attractive van der Waals interactions as well as repulsive double-layer forces.

- Surface charge/potential is assumed to be uniformly distributed. Charges are discrete by nature, however, and electrical properties of colloidal particles therefore vary on a microscopic scale. Such heterogeneous distributions of surface charge/potential could affect the magnitude of repulsive double-layer interactions.

- DLVO theory does not consider interactions involving the solvent, which is treated as a continuous homogeneous medium characterized by a single value of the dielectric constant. Such interactions could arise, however, if the solvent is polar [as is $H_2O(l)$]. For aqueous systems, these interactions may include hydrogen bonding, hydrogen donor/acceptor reactions, hydration and steric interactions. The result of such interactions is a re-structuring of water in layers adjacent to the solid's surface.

- Ions in the diffuse layer are assumed to be point charges, *i.e.*, the sizes of the ions are ignored. This assumption is not valid when the separation distance between colloidal particles is small and the surface potential is high. Under such conditions, the numbers of ions in the diffuse layer calculated using DLVO theory are far too large.

- Repulsive and attractive forces between colloidal particles are assumed not to vary with time. In reality, however, the total interaction energy between particles may fluctuate due to a redistribution of charge in the double layer or solid by diffusive or conductive mechanisms, or during particle rotations as a result of irregular particle shape and/or heterogeneities in surface charge.

Swanton (1995) and Jansson (2007) describe efforts to deal with these limitations. These efforts have resulted in the formulation of various "extended" DLVO models. The extended models provide more accurate descriptions of

colloidal systems, but come at the expense of an increased number of model parameters that must be characterized experimentally.

There are additional limitations in DLVO theory when it is applied specifically to colloidal systems of clay minerals (Stumm and Morgan, 1996; Liu and Neretnieks, 2006). One limitation stems from the fact that these minerals carry a net negative charge on faces oriented parallel to the dominant tetrahedral-octahedral-tetrahedral layering, and, depending on pH, net positive or negative charges on edges that are oriented normal to this layering (*e.g.*, Grim, 1968; see Section 2.2). This means that a given clay particle can have different double-layer structures associated with its faces and edges. Particle-particle interactions in clay colloidal systems may consequently involve face-to-face (FF), edge-to-face (EF) and edge-to-edge (EE) interactions. Because the EF interactions involve particle surfaces of unlike charge, particle agglomeration may occur even in dilute electrolyte solutions. The DLVO model does not account for such interactions, and may thus overestimate the stability of clay colloids.

The DLVO model also does not account for the effects of specific adsorption on colloid stability (Boström *et al.*, 2001). The model assumes only that the electrolytes in a colloidal suspension are inert, and that their effect on colloid stability is through the control on double-layer thickness represented by the reciprocal of the Debye parameter, κ (Section 3.3). Other electrolytes in clay colloidal systems may form covalent complexes with functional groups at the particle's surface, however (*e.g.*, Langmuir, 1997). Such complexes alter the surface charge and surface potential, and thereby affect colloid stability. H^+ and OH^- are important potential-determining ions because they react with the surface sites of clay minerals. The colloidal stability of these minerals is thus pH-dependent, but this dependency is not accounted for in DLVO models (Missana and Adell, 2000).

2.1.4.1 Effects of clay composition on stability relations among sols, gels and flocs

Kjellander *et al.* (1988) used a statistical mechanical approach to evaluate double-layer interactions involving clay minerals. Counter to expectations based on DLVO theory, the interaction energy between like-charged clay surfaces was found to be strongly attractive at relatively small inter-particle separation distances if the counterions in the diffuse layer were divalent and if the surface-charge density was large (as is true generally for smectites, including montmorillonites).

This additional attractive force was attributed by Kjellander *et al.* (1988) to ion-ion correlations (see also Janiak *et al.*, 2008; Pegado *et al.*, 2008). The correlations involve repulsive interactions among ions of like charge, which in effect create a "hole" of charge depletion around each ion. The charge-depletion region around an ion can be regarded as a charge-accumulation region of opposite sign. The interaction of an ion on one side of the mid-plane between two colloidal particles (*e.g.*, at $d/2$ in Figure 2.1.3.3_1) with an ion and part of a charge-depletion hole on the other side of the mid-plane creates an attractive force between the particles that is not accounted for in

classical DLVO theory. This attractive force, together with the van der Waals force, is not large enough to counteract the repulsive force between two clay particles when the counterions are monovalent, but can counteract this repulsive force when the counterions are divalent and the surface-charge density is high.

The attractive force due to ion-ion correlations is apparently important for montmorillonites having exchangeable Ca/Na molar ratios greater than about 90/10 (*e.g.*, Birgersson *et al.*, 2009). In such cases the attractive force is sufficiently strong that the minerals cannot expand to form gels or sols. On the other hand, montmorillonites having Ca/Na < 90/10 can form gels or sols depending on whether counterion concentrations exceed the CCC. This is important from the viewpoint of buffer erosion because it suggests that buffer materials composed of essentially pure Ca-montmorillonites would be much more resistant, if not completely impervious, to the effects of chemical erosion than buffer materials composed of mixed Na/Ca-montmorillonites having Ca/Na < 90/10 (*e.g.*, MX-80).

2.2 Clay colloid formation and stability

2.2.1 Structure of clays

Clays have a layered structure based on a 2-dimensional covalent network of tetrahedral SiO_4 units, Al units of varying coordination and sometimes also divalent cations. For most clay minerals, these layers, with a thickness around 1nm, carry a net negative charge. In a water-free system, the negative charge is compensated by cations in the space between the layers as illustrated in Figure 2.2.1_1.

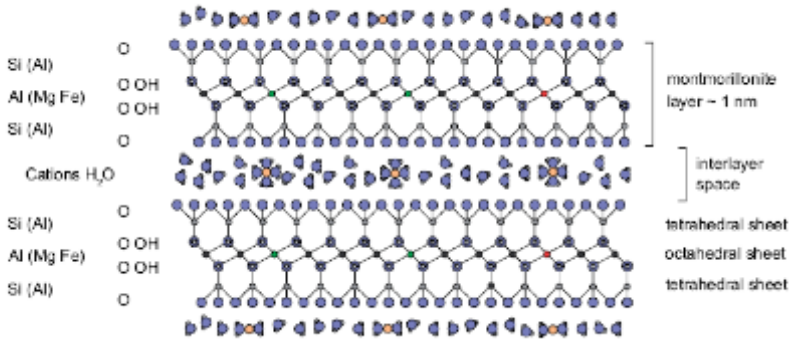

Figure 2.2.1_1: The structure of montmorillonite containing a two-dimensional covalent network of Si, Al and O forming layers approximately 1nm thick and which are separated by cationic counterions and possibly water (SKB, 2006b).

When exposed to water, or an electrolyte solution, a swelling of the layers can occur and, in the extreme case, the swelling into excess water results in separated layers. In practice, the layers have a finite size in the lateral direction and the highly swollen system is a stable solution of flake-like colloidal particles. The layer thickness is approximately 1 nm, while the lateral exten-

sion of the layers depends on the history of the particular clay system. In addition, the chemical nature of the edges is not well-defined and can vary from clay to clay, even if their nominal compositions are the same.

In the dispersed state, the clay particles have a negative charge, which is compensated by counterions in the electrical double layer. Typical charge densities on the flat surfaces of montmorillonite are in the range 0.10 to 0.15 C m^{-2}. This is a rather high charge density compared to other colloidal systems, and approximately corresponds to one elementary charge, per 100 to 150 $Å^2$. On the edges the charge is more variable, but it can be positive at neutral pH. The edge charge appears to be pH sensitive around neutral pH, while the charge density on the flat surfaces only appears to titrate at lower pH (Wieland, *et al.*, 1994; Evans and Wennerström, 1999). However, one should be aware of the fact that a dilution by pure water changes the titration equilibrium such that a protonation of the surfaces can occur at lower pH-values.

Montmorillonite clays, and other swelling clays, can be viewed as occurring in three different forms depending on conditions. If water availability is limited, either physically or chemically, the original clay mineral swells to a state with a finite distance between layers. Sheets are basically parallel and with a uniform spacing between layers. A typical sample has a polycrystalline character with domains of ordered packed layers of different orientation meeting in defect zones. In the other extreme, where water is plentiful, the system swells to high dilution with individual, essentially uncorrelated, particles. When such a system is exposed to higher concentrations of electrolyte, an aggregation can occur that leads to the formation of a disordered network of contacting particles. In comparison to the layered structures, such networks occupy a larger volume per dry weight of clay.

2.2.2 Electrostatic interactions

The simplest model relevant for clay systems is one of uniformly charged surfaces separated by a solvent layer containing only neutralizing counterions. In the so-called primitive model, the solvent (water) is represented as a medium with a dielectric permittivity representing the properties of the pure solvent. Ions are considered spherical with a hard-core radius. Figure 2.2.2_1 gives an illustration of the model. The model can easily be extended to include an electrolyte with either a specified concentration or a case where the electrolyte concentration is determined by an equilibrium with a bulk solution of specified (bulk) concentration.

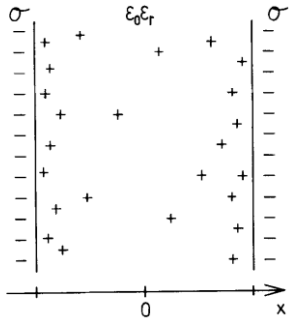

Figure 2.2.2_1: Negatively charged layers of uniform charge density σ separated by a medium of permittivity $\varepsilon_r\varepsilon_0$ with counterions of charge +e.

The most common and convenient theoretical description of this model system is based on the Poisson-Boltzmann (PB) equation. It is a mean field approximation in which the lateral ion distribution is described in terms of the mean distribution. For the counterion only case, there is a simple analytical solution of the PB equation (Engström and Wennerström, 1979). For the case when there is also electrolyte present, the solution is more involved (Verwey and Overbeek, 1948). A discussion of the relation between the two solutions is given by Jönsson and Wennerström (1980). For the counterion only case, the PB equation predicts that there is a repulsion between layers that is inversely proportional to the separation. In the presence of electrolyte, the repulsion decays exponentially at long range with a decay length given by the Debye screening length. At shorter separations there is a gradual transition to the counterion only case. In this theoretical description, the difference between monovalent and divalent counterions is quantitative. The divalent counterions produce a smaller repulsion than the monovalent ones, as is evident from the smaller decay lengths obtained with divalent ions at the same concentrations.

There are basically two possible strategies for improving the description of the interaction between two colloidal particles using the PB equation. One possibility is to make the model more physically realistic by accounting for the solvent's dielectric properties explicitly, rather than treating the solvent as an idealized, uniform dielectric medium. The other alternative is to continue using the primitive model, but then solve the statistical-mechanical problem in a better way.

It is technically rather difficult to find a method where one explicitly accounts for the solvent effects. So far this hasn't been accomplished for water-like systems, but it has been done for simpler solvents with a clear dielectric screening effect. Such studies show that the effect of the ion-ion correlations discussed above remains. The primary effect of the solvent is that the interaction becomes oscillatory at short range, where the characteristic distance is determined by the size of the solvent molecules. Figure 2.2.2_2 shows typical calculated force curves demonstrating the effect.

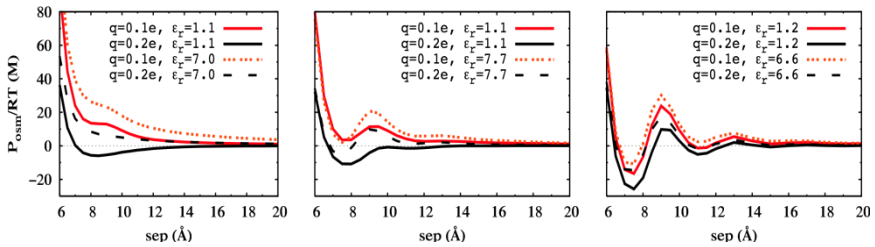

Figure 2.2.2_2. Monte Carlo calculations comparing the force per area between plates for the cases of a solvent as a dielectric medium, left panel, and two cases where the solvent is represented in terms of molecules (dipolar spheres). Middle panel = medium dipolar density; right panel = high dipolar density. The oscillations in the force curve are for these two cases caused by packing of solvent molecules. (From Pegado *et al.*, 2008).

An improved statistical-mechanical description of colloidal systems has been developed using Monte Carlo computer simulation techniques (Guldbrand *et al.*, 1984) applied to the inhomogeneous hypernetted chain (HNC) equation (Kjellander and Marçelja, 1984). An important result of these studies, in the present context, is that for highly charged systems such as montmorillonite colloids, the PB equation can fail even to correctly predict conditions under which the colloids are stable or unstable. Such failure occurs because the PB equation does not account for the ion-ion correlation effects discussed above. These effects can be important for colloidal systems with divalent counterions in water because the force curve becomes non-monotonic around a charge density of 0.07 C m^{-2} and a net attraction, relative to infinite separations, occurs for charge densities above 0.09 C m^{-2}. For monovalent counterions, sizable corrections to the PB results are only needed at very high charge densities (> 0.3 C m^{-2}).

2.2.3 Swelling properties of clays

When a layered clay material is in contact with H_2O in the form of pure water, an aqueous solution, or as a vapour in air, the clay tends to incorporate H_2O molecules and swell. The extent of swelling depends on the nature of the clay, on the chemical potential of H_2O and on the possible presence of other substances such as electrolytes that can enter or interact with the clay . There are, in general, five different scenarios for the swelling behaviour:

- the clay is unaffected, as is the case for mica;
- there is a limited swelling in which adjacent clay surfaces are separated by one or two well-defined layers of solvent (“crystalline swelling”);
- the clay swells to a finite thickness, which varies depending on conditions in the aqueous phase;
- the swelling occurs in a finite system, and an equilibrium is established between two different extents of swelling; and
- the clay swells indefinitely, ultimately forming a stable dilute sol.

Which of these scenarios occurs for a specific case is basically determined by the net force acting between the layers of the clay. The swelling pressure is given by the difference between the osmotic pressure between the layers and the osmotic pressure (or the equivalent water chemical potential) in the surrounding reservoir. Formally one can write the swelling pressure as:

$$p_{swell} = \frac{force}{area} = \Pi_{osm}(layer) - \Pi_{osm}(reserv), \qquad (2.2.3\_1)$$

where Π_{osm} is the osmotic pressure.

In the standard DLVO theory (see Section 2.1.3), the osmotic pressure of the layer results from an electrostatic repulsion, described by the PB approximation, and an attraction caused by the van der Waals interaction. For an ordered system with layer separation, *h*, and layer thickness, *L*, one has:

$$\Pi_{osm}(layer) = k_B T \sum_i c_i\,(mid\_plane) - \frac{A}{6\pi}\left\{\frac{1}{h^3} - \frac{2}{(h+L)^3} + \frac{1}{(h+2L)^3}\right\}, \qquad (2.2.3\_2)$$

and the osmotic pressure in the reservoir is that of an ideal, bulk salt solution:

$$\Pi_{osm}(reserv) = k_B T \sum_i c_i\,(bulk). \qquad (2.2.3\_3)$$

The summation in the latter two equations extends over all ionic species, *i*, in the system, and concentrations, *c*, are measured in terms of the number of ions per unit volume. For simple systems, the force curve represented by Equations (2.2.3_1) to (2.2.3_3) has a minimum at small values of *h* (note that *h* is also bounded by a minimum allowed value). At intermediate separations the first, repulsive, term typically turns the swelling pressure positive, while it asymptotically approaches marginally negative values again at very large separations. In highly compacted clays such as the bentonite buffer, the clay minerals will be so highly charged, and the thickness, *L*, so small, that electrostatic interactions will dominate the van der Waals attraction, and the swelling pressure will be strongly positive.

Focusing on the electrostatic interactions, the swelling scenarios discussed above can be interpreted as follows.

- Non-swelling clays have such a strong cohesion caused by ionic and dipolar interactions that the swelling pressure is strongly negative at small separations. If separated, by a mechanical cleaving, they be-

have to a large extent as swelling clays, as illustrated by the large body of experiments on mica systems (Israelachvili and Adams, 1978).

- Clays that exhibit "crystalline" swelling have a weaker short-range cohesion, while the oscillations in the force curve, due to the size of solvent molecules, that always exists for "hard" surfaces produces minima that are deep enough to prevent swelling beyond the first or second minimum (see Figure 2.2.2_2 for an illustration).

- A clay (with charged layers) that swells indefinitely follows what is expected from the predictions of the PB equation.

- To understand under which circumstances there is only a limited swelling of the layers, one can note that this primarily occurs for the case when divalent ions dominate in the system. With the charge densities typical for the montmorillonite clays it has been conclusively shown that the mathematical approximation leading to the PB equation breaks down and one should expect an attractive, or close to attractive, behaviour for the force between the layers. With such an attraction the layered clay system should be in equilibrium with a dilute aqueous phase. At this phase boundary the swelling pressure is zero.

- It is interesting to note that for the typical bentonite clay systems considered for use as "buffers" in geological repositories for nuclear waste, the estimated charge density is just slightly higher than the theoretically predicted limit for transition from attractive to repulsive behaviour when divalent ions act as counterions (Guldbrand *et al.*, 1984). As was also shown, the transition from a clearly attractive state to a monotonically repulsive one occurs with the appearance of a non-monotonic force curve. For a system of a finite clay concentration this can result in a coexistence between two fractions with very different water contents at equilibrium (for an experimental example of this behaviour in a charged layer system see Khan *et al.*, 1985). In a system swelling under non-equilibrium conditions one expects, under these circumstances, an abrupt change in concentration at some distance into the clay material.

2.2.4 Ion exchange

In most cases of practical relevance, clays swell in an aqueous system containing several different kinds of cations. There is always a selectivity in the uptake of ions and, at equilibrium, there can be quite a different net ion concentration in the clay material relative to bulk values. There are two kinds of selectivity. One operates between different cations of the same valency. This is caused by the short-range interaction between the counterion and the clay sheet. Even though this selectivity can be substantial between cations of clearly different size, it is of lesser relevance for the buffer erosion problem since sodium and calcium are projected to be the dominant monovalent and divalent ions, respectively. The primary cause of Na^+ versus Ca^{2+} selectivity

is electrostatic. For highly charged systems with low electrolyte concentrations in the reservoir, there will be a very strong preference for uptake of calcium into the aqueous layer between the charged surfaces of the clay. When modelling this effect, one has to explicitly account for the electrostatic interactions. Within the PB description, the concentration profile between sheets is given by:

$$c_i(z) = c_i(bulk)\exp\left(-\frac{z_i e\psi(z)}{k_B T}\right), \qquad (2.2.4\_1)$$

where the reference position for the electrostatic potential is in the bulk of the solid clay. The total amount of ion *i* per unit surface is then:

$$\frac{n_i}{area} = \int_{-\frac{d}{2}}^{\frac{d}{2}} c_i\,(z)dz. \qquad (2.2.4\_2)$$

Although the PB expressions given above can be used to estimate ion concentrations for the case when correlation effects are important, it is necessary to explicitly include the correlation effects to achieve quantitatively accurate numbers . One can note that the selectivity:

$$\frac{n_{Ca}/c_{Ca}(bulk)}{n_{Na}/c_{Na}(bulk)} \qquad (2.2.4\_3)$$

depends on both the total ion concentration and the layer separation, *h*, for a given charge density. For sub-mM bulk electrolyte concentrations, the clays can have very strong preferences for the divalent ions as compared with monovalent ions (see Evans and Wennerström, 1999; p. 142).

When the composition of the aqueous system surrounding the clay changes, there will be an exchange of ions in the water/clay system. For a clay material of 1 meter thickness a simple estimate based on diffusional transport predicts that the equilibration time will be of the order 100 years, which is a long time in most contexts, but not in relation to the timescales of interest in radioactive waste disposal.

2.2.5 Precipitation of a clay sol

Once dispersed into a thermodynamically stable sol, a clay gel can be precipitated by the addition of, for example, NaCl to give a high bulk concentration. Experiments reported by Birgersson *et al.* (2009) indicate that for the

clay systems of interest here, a concentration exceeding 25mM is sufficient to cause precipitation and formation of a percolation gel. A study of this effect is of interest for a general understanding of clay behaviour, but it is worthwhile emphasizing that once the clay particles have formed a dilute sol, they are likely to be carried away by groundwater flow before conditions change to non-swelling conditions. Thus, precipitation phenomena are not discussed further here.

2.3 Summary of relevant experimental observations

This section discusses some recent experimental work performed by SKB and its contractors to investigate buffer erosion. This discussion has been made by considering the experimental conditions investigated, the experimental set-ups used, and the interpretations of the experimental results made by SKB and its contractors.

A key area of interest has been on determining the extent to which the experiments performed are reliable and support the conceptual models described by SKB.

Given the conceptual models described by SKB and its contractors (*e.g.*, Neretnieks *et al.* 2009), the focus is on if and how bentonite from the buffer moves into and subsequently behaves in fractures in the host rock.

Key experiments that have sought to investigate this area include:

- glass slit tests (Neretnieks, 2009);
- artificial fracture tests (Jansson, 2009); and
- erosion tests (Birgersson *et al.*, 2009).

Comments regarding each of these types of experiments are summarized below.

2.3.1 Glass slit tests

Neretnieks (2009) investigated the behaviour of four different bentonites in a water filled artificial fracture formed using two vertical glass plates (Figure 2.3.1_1). The glass plates were 180 by 130 mm in size and the fracture formed between the two plates had an aperture of 1.3 mm.

The bentonite was initially added as a layer at the bottom of the fracture. This was allowed to settle and swell, and then the fracture was inverted so that the bentonite layer was at the top of the fracture (Figure 2.3.1_1).

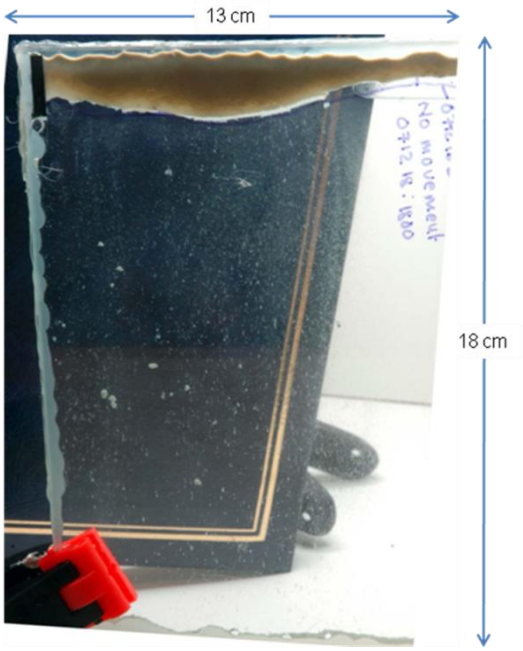

Figure 2.3.1_1. Artificial water-filled fracture formed from two glass plates with a layer of brown bentonite between the plates at the top (Neretnieks, 2009).

The four clay materials used in the experiments were:

- MX-80.
- MX-80 that had been washed to remove gypsum[7].
- Na-MX-80 with no accessory minerals.
- Ca-MX-80 with no accessory minerals.

Observations made for the untreated MX-80 system included (Neretnieks, 2009):

- Below the Critical Coagulation Concentration (CCC), bentonite gel can be pulled apart by gravity to form blobs with enclosed accessory minerals - these settle downward through the fracture.
- Large blobs, which span the aperture of the fracture, are retarded by friction on the walls; small blobs (above colloidal size) sediment rapidly.
- The dimensions of the fracture influence the formation of the gel blobs and their sedimentation rate.

[7] The washing process actually removes gypsum and clay, and so yields a material with a relatively high concentration of accessory minerals.

Observations made for the experiments with MX-80 that had been washed to remove gypsum included (Neretnieks, 2009):

- The washed material does not rapidly disintegrate into a stable sol, even if the porewater concentration is below the CCC.

- Blobs and '*worms'* of gel can be pulled apart by gravity and sediment downwards (Figure 2.3.1_2).

- '*The outer rim of the swollen gel can separate into a clear, thin gel and a more concentrated gel containing the detritus material*' (Figure 2.3.1_3).

Based on the latter observation, Neretnieks *et al.* (2009) suggested that '*a tentative interpretation is that as the gel expanded upwards the detritus material expands with it, but near the edge where the gel density had decreased the smectite particles could move independently of the detritus leaving it behind. In this case, half a mm thick region of more concentrated detritus remained forming a potential filter cake*.'

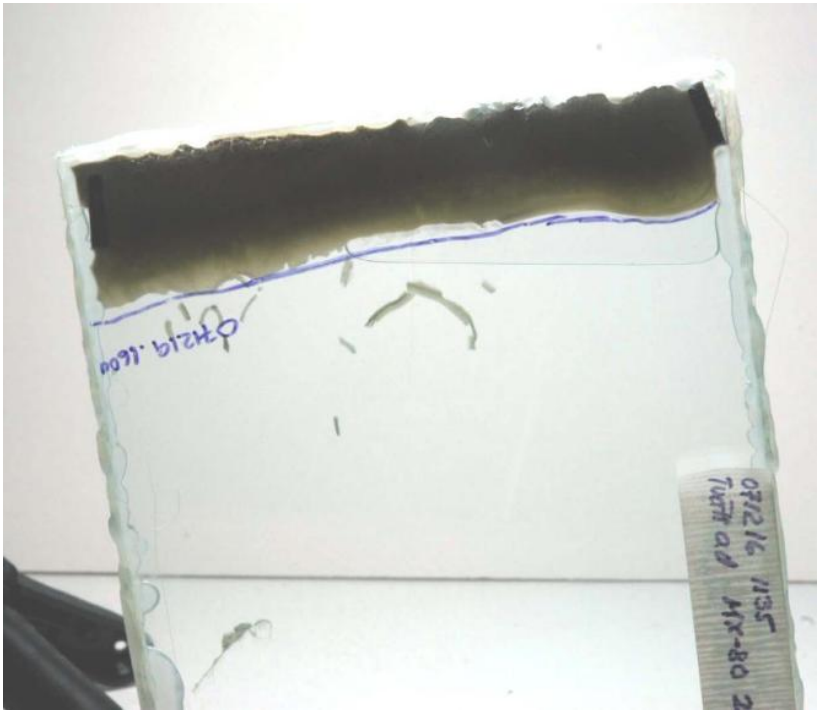

Figure 2.3.1_2. Artificial water-filled fracture formed from two glass plates with brown bentonite between the plates at the top, showing the formation and settlement of blobs and worms of bentonite (Neretnieks, 2009).

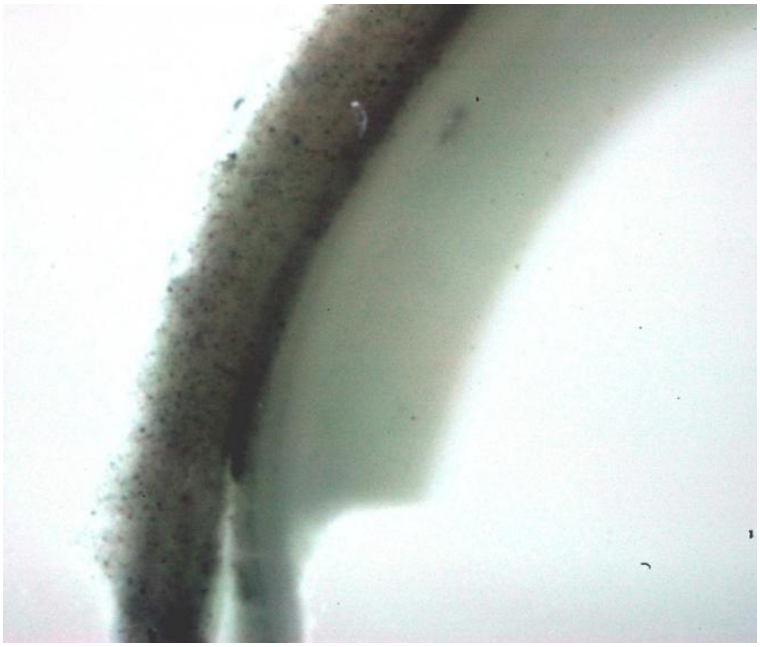

Figure 2.3.1_3. **Close up of the bentonite gel worm of Figure 2.3.1_2 showing variation in the amount of dark accessory minerals (Neretnieks, 2009).**

Our evaluation of these experiments is that they are rather simple scoping experiments (this is acknowledged by the authors) in which conditions were not tightly controlled. The glass plates do not provide a good representation of a real fracture of the type and dimensions likely to be found in the repository host rock. In particular, the aperture of the fracture was rather large and the results of the experiments on the settling behaviour of the bentonite clay blobs etc. were clearly influenced by the experimental set-up. The experiments do, however, illustrate the effects of gravity on clay gels and demonstrate that settling of relatively large clay particles (well above the colloidal size range) does occur.

Neretnieks *et al.* (2009) claim that the accessory minerals in the bentonite material could slow the expansion of smectite towards the gel/water interface. The evidence presented for this is not clear, and the interpretation of the experiments as showing the formation of a potential filter cake is unconvincing.

The experiments on the system with Na-MX-80 and no accessory minerals failed because of leaks and air bubbles. Also, some anomalously high Ca concentrations were observed that were hard to explain given that the bentonite was a Na-exchanged type.

Observations made in experiments on the system with Ca-MX-80 and no accessory minerals showed aggregation and settling of clay aggregates in waters of ~1 mM Ca, which SKB assumes to be close to the CCC.

2.3.2 Artificial fracture tests

Jansson (2009) described some more elaborate experiments, this time with an experimental set-up designed to represent bentonite swelling and erosion in a horizontal fracture (Figure 2.3.2_1). Bentonite that had been washed to remove gypsum was compacted to a density of 1000 Kg m^{-3} in a container attached on one side of a 0.1 to 1.0 mm wide fracture, through which distilled water was pumped. The bentonite container had a separate water supply that was used to saturate the bentonite.

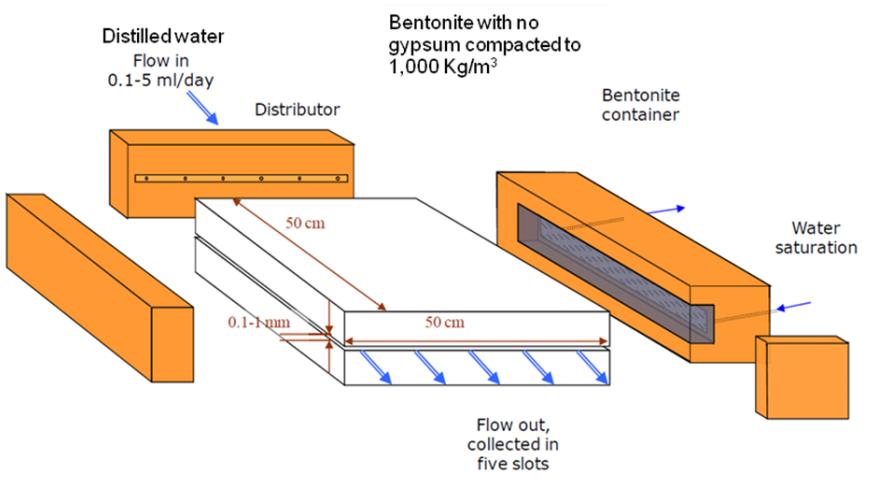

Figure 2.3.2_1. Diagram of the experimental set-up for the artificial fracture tests of Jansson (2009).

Two experiments were conducted; the first with a truly horizontal fracture and the second with the fracture inclined by 2 to 3 degrees down towards the inlet in order to try to allow some air bubbles that had formed to escape to the outlet.

Photographs of the experiments are shown in Figures 2.3.2_2 and 2.3.2_3, which have been annotated to highlight key aspects. The photographs are taken from directly above the horizontal fracture and are oriented so that the water flow through the fracture appears to be down the page and the bentonite appears to be swelling out of its container into the fracture from the right hand side of the page.

The first experiment (Figure 2.3.2_2) shows the erosion of bentonite and the dispersion of bentonite colloids and particles, described by Jansson (2009) as a sol, into the water flowing in the fracture. Also seen in this experiment is the development of a discontinuous layer of darker and relatively feldspar-rich material close to the bentonite gel/sol interface.

The second experiment, having a slightly inclined fracture, illustrated some further processes in addition to those observed during the first. As well as bentonite swelling, bentonite erosion and the formation of a discontinuous

layer of darker and relatively feldspar-rich material close to the bentonite gel/sol interface, dispersed bentonite was seen to move within the fracture towards the flow-inlet side of the fracture under the influence of gravity (Figure 2.3.2_3). The dispersed bentonite affected the water flow pattern, which became channelled, as shown by the use of blue dye (Figure 2.3.2_3).

The concentration of colloids at the fracture outlet is quoted as being < 0.18 g l^{-1}, and the colloids reaching the outlet were measured as < 200 nm in size and mostly < 100 nm in size (Jansson 2009).

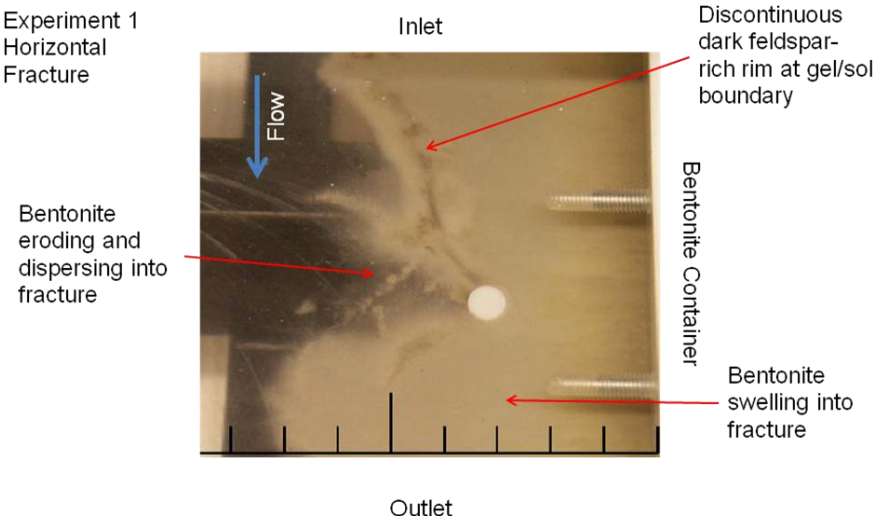

Figure 2.3.2_2. Annotated photograph of the first artificial fracture tests of Jansson (2009).

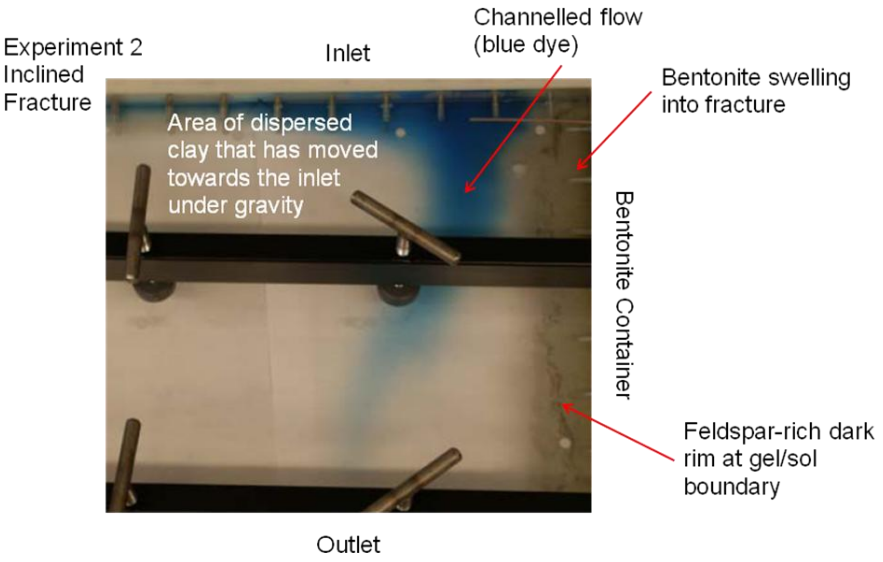

Figure 2.3.2_3. Annotated photograph of the second artificial fracture tests of Jansson (2009).

These experiments have produced some interesting observations on the processes that can occur as bentonite swells and is eroded in a fracture. As noted above in respect of the scoping experiments reported by Neretneiks (2009), this experimental set-up still does not provide a good representation of a real fracture of the type and dimensions likely to be found in the repository host rock. However, the observations of complex, time varying water flow patterns through fracture areas that become filled with dispersed bentonite is potentially important, and various similar effects (*e.g.*, fingering) might be envisaged. These effects are not included in the conceptual models described by SKB and its contractors (*e.g.*, Neretnieks *et al.* 2009).

In more detail:

- The density of the bentonite in the experiments was lower than is planned for the waste deposition holes in the repository, and so in this respect the experiments may give the impression of less bentonite swelling (and possibly less bentonite erosion) than may occur in the repository system.

- The experiments were conducted with initially pure distilled water and the solution chemistry was not well constrained. The experiments may, therefore, give the impression that bentonite erosion is more likely and extensive than may actually occur in a repository system with more saline and/or Ca^{2+} rich groundwaters.

- The experiments were conducted with atmospheric levels of CO_2, which will have influenced the solubility of calcite, the concentrations of Ca^{+2} in the waters, and possibly had an effect on the stability of the clay colloids.

- One of the two experiments suffered from air bubbles. There is evidence that in two phase aqueous systems, colloids may adhere to, or collect at, the gas water interface (*e.g.*, Bennett *et al.*, 1998) and so it is important that a technical solution is found for keeping future experiments air/gas free.

- The absolute concentrations of colloids measured in the outlet solutions are of questionable relevance to the repository system.

2.3.3 Erosion tests

Birgersson *et al.* (2009) described some experiments focussed directly on measuring the erosion of bentonite. In these experiments, various ionic solutions were circulated past bentonite clay samples and the swelling pressures exerted and the turbidity of the circulating solutions measured.

Changes were made to the composition and salinity of the solutions during the experiments, and bentonite erosion was evidenced by a drop in swelling pressure and an increase in solution turbidity.

The experimental set-up is shown in Figure 2.3.3_1.

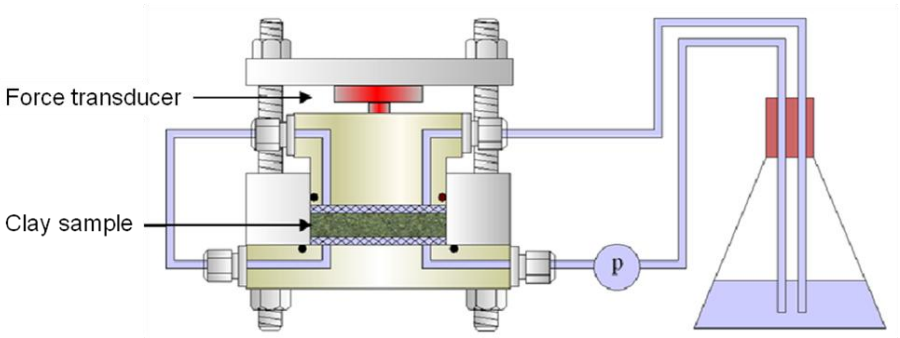

Figure 2.3.3_1. Diagram of the experimental set-up for the bentonite erosion tests of Birgersson *et al.* (2009).

The clay materials used in the experiments were:

- Pure Na-montmorillonite.
- MX-80 that had been washed to remove gypsum.

The solutions used in the experiments were:

- $CaCl_2$.
- Mixtures of $CaCl_2$ and NaCl.
- $CaSO_4$.
- $CaCO_3$.
- Pure water.

Example results from these experiments are shown in Figure 2.3.3_2.

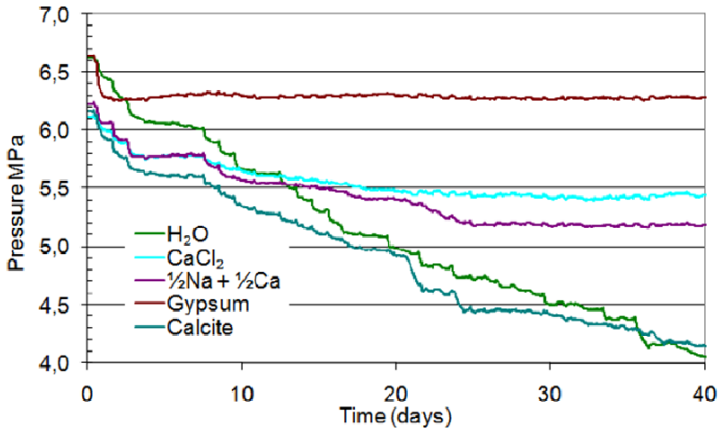

Figure 2.3.3_2. Swelling pressures measured on Na-montmorillonite samples exposed to different circulating waters (Birgersson *et al.* 2009).

The results indicate that (Birgersson *et al.*, 2009):

- Erosion does not occur in the presence of gypsum, presumably because gypsum dissolution causes the concentration of Ca^{2+} in the circulating solution to be high enough to destabilise any colloidal suspensions. Measured concentrations of Ca^{2+} in these solutions are ~16 mM.

- Erosion of Na-rich montmorillonite stopped when a solution of 5mM NaCl and < 2.5 mM $CaCl_2$ was circulated.

- Erosion of MX-80 with no gypsum stopped when a solution of 0.7 mM NaCl and 0.2 mM $CaCl_2$ was circulated.

These experiments have provided a limited number of useful observations on some specific chemical conditions which may prevent bentonite erosion but, because of the experimental set-up, they have not provided information on physical erosion of bentonite. This is because the bentonite samples are held physically in the apparatus by metal gauze or filters.

With regard to quantifying the amount of bentonite erosion, it is not clear if the observed changes in swelling pressure result solely from erosion, or whether some of the changes are due to changes in solution chemistry.

One other observation on these experiments is that it would have been better if the final ion contents of the clays and the waters had been measured instead of being inferred from ion-exchange calculations.

3. Physical aspects of buffer erosion

3.1 Modelling perspective

The primary purpose of modelling in general is to improve and quantify our understanding of the effects of various processes occurring under certain circumstances and conditions. How well our models really describe or quantify the problem at hand depends on the assumptions made and data used in solving the problem. Models of buffer erosion, specifically, require consideration of a number of physical sub-processes, which are briefly discussed in this chapter.

The scenario dealt with here involves the removal of bentonite by water flowing in fractures in the bedrock surrounding a KBS-3 repository (see Figure 1_1). The question of concern is how much bentonite might be removed over a certain time interval. The processes involved are based on the assumption that bentonite intrudes into the fractures due to its swelling pressure, *i.e.*, radial transport of bentonite relative to the deposition hole. At the swelling front flowing water erodes the bentonite, *i.e.*, tangential transport relative to the deposition hole. This might result in further expansion of the bentonite, followed by further erosion.

This problem has been dealt with by SKB mainly in two reports by Birgersson *et al.* (2009) and Neretnieks *et al.* (2009). In the following sections the different assumptions made in the respective analyses and interpretations presented in these reports are identified, described and discussed. The focus is on simplifications made regarding geometry and rheology (geotechnical soil parameters and flow properties). Furthermore, the extent of experimental back up information is discussed and also the uncertainties are, if not quantified, at least qualitatively dealt with in relation to their importance for the results.

3.2 Assumptions

The evaluations carried out by Birgersson *et al.* (2009) and Neretnieks *et al.* (2009) are based on a number of assumptions. Several of these assumptions are considered in detail below. It is important to identify and clearly state all the assumptions made, as otherwise different hidden assumptions, which might be important, might be overlooked and not given due attention.

3.2.1 Geometry

In reality, fractures are three-dimensional, irregular and with varying dimensions, not always continuous, and with lots of residual material (*e.g.*, minerals) deposited or chemically formed, see Figure 3.2.1_1a. Close to the repository, in the EDZ, they might be larger, but further away, in the original

state of the bedrock, the fractures are probably much smaller and less varying in thickness. This irregular geometry is not suited for analytical modelling and therefore a straight, continuous, two-dimensional fracture plane with a constant thickness is usually assumed, see Figure 3.2.1_1b.

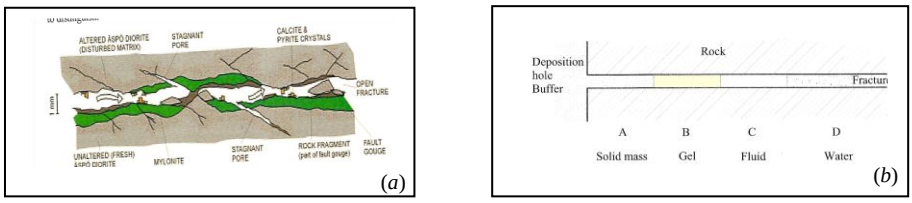

Figure 3.2.1_1. Fractures considered (*a*) in the prototype and (*b*) conceptual models.

3.2.2 Material phases

As the bentonite swells it gradually transforms from a *solid mass* to a *gel*, and after further swelling the gel gradually transforms to a *fluid (sol)* and eventually after extensive swelling it can be regarded as *water* with suspended particles (see Figure 1_1). During this transformation, the water content increases tremendously and, thus, different models for material behaviour need to be used for the different phases. The terminology used for the different phases is not obvious and also needs to be clarified (the terminology adopted in the present report is summarized in Section 1.3).

The chemical composition of the bentonite, clay mineralogy (including accessory minerals), as well as the intruding water have a tremendous effect on the processes that will govern expansion and possible erosion.

3.2.3 Geotechnical parameters

When the bentonite expands and intrudes into an aperture, the expansion may be counteracted or balanced by the shear strength of the material in combination with wall friction. In geotechnical engineering a vast number of constitutive models for the shear strength of soil exists, but the most common is the Mohr-Coulomb failure hypothesis. The material is assumed to be an ideal elasto-plastic material and two parameters, φ' and c' define the shear strength, τ_f , as:

$$\tau_f = c' + \sigma' \tan \varphi'.$$

Another way of expressing the shear strength is by a fixed value, $\tau_{fu,}$ (the undrained shear strength), linked to a given water ratio, and the stress-strain properties are then defined as a working curve.

Wall friction is usually expressed as a ratio, r, of the friction along the wall, tan δ, to the shear strength

$r = \tan \delta / \tan \varphi'$ or $r = \tau_{mobilized} / \tau_{fu}$

In most geotechnical cases, the strength parameters c', φ' and r are assumed to be constant over the entire stress field, that is for all values of σ'.

It is, however, possible that the shear strength parameters and, thus, also the wall friction will vary with the effective stress. These assumptions, regarding the shear strength parameters and the wall friction, have great implications for the length of the intrusion of the bentonite into an aperture.

3.2.4 Flow properties

Because the bentonite is expansive it will exert a swelling pressure if the expansion is restricted by a rigid boundary. If there is an opening, a crack, in the boundary, the bentonite will expand into that opening. This flow of material out into the crack needs to be modelled, and therefore a model for the flow properties, usually referred to as rheology, of the material must be adopted. This part of material behaviour has been comprehensively studied, *e.g.* within the research area of grouting. The most common and widely used models are briefly described in Figure 3.2.4_1 and 3.2.4_2.

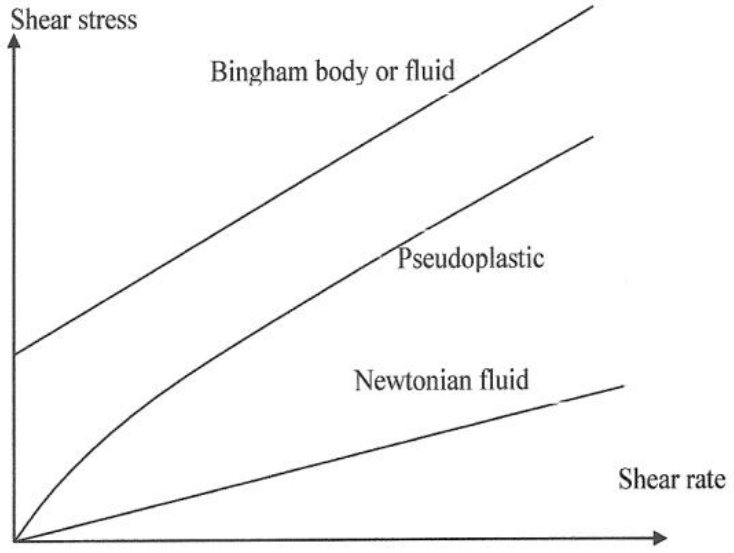

Figure 3.2.4_1. Schematic diagram illustrating relations between shear stress and shear rate governing Newtonian, Pseudoplastic (power-law) and Bingham flow behaviour.

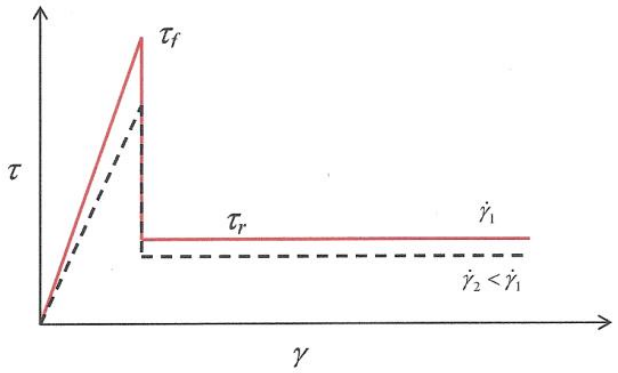

Figure 3.2.4_2. Schematic diagram illustrating stress-strain relations in bentonite.

The rheological models are defined by the governing equations, and by assigning values to the relevant parameters, the behaviour of the material is defined over a wide range of flow rates.

The flow properties described above are simplifications and true material behaviour is complicated by, for example, thixotropy.

3.2.5 Geochemical aspects

The geochemical aspects of buffer erosion are extremely important and complicated, but are dealt with separately in this report (see Sections 2.1, 2.2 and 4).

3.3 Experimental backup - verification

SKB and its contractors have used two different approaches for constitutive modelling. They are referred to here as the Clay Technology (CT) model (Birgersson *et al.*, 2009), and the Kungliga Tekniska Högskolan (KTH) model (Neretnieks *et al.*, 2009). These two models are dealt with separately below. It is important to realize the spectrum of different densities or water contents for the material in different phases and, thereby, the vast differences in material properties and, thus, also to appreciate the difficulties associated with determining these properties experimentally.

On one end the bentonite is highly compacted with a density around 2000 kg m^{-3}, partly saturated with a water content (or water ratio, see Section 1.3) of 0.1. As it swells the density gradually decreases, the material is assumed to be saturated and the water content increases by several orders of magnitude and becomes 100 or even 1000. Eventually it constitutes water with suspended bentonite particles. It is also worth bearing in mind, as many of the results presented are given in Pa, or even fractions of a Pa, that 1 Pa corresponds to the pressure exerted by a column of water 0.1 mm, or 100 μm, high.

Apart from the water content, different clays will behave differently and perhaps even more important is the chemistry of the water, *e.g.* presence of different ions and in what concentration. This will complicate and expand the necessary testing program.

3.3.1 CT model

SKB's constitutive model is rather straightforward and, to a certain extent, typical of modelling often undertaken by researchers having material behaviour as a base (see Birgersson *et al.*, 2009).

A simplification of the geometry to a two-dimensional, highly idealized fracture with a constant width is utilized and the only parameter needed to describe the fracture is the aperture width.

The parameters needed for describing the swelling of the clay, strength and flow properties of the expanding clay, interaction with the aperture walls etc., have to a certain degree been determined by rather comprehensive laboratory testing programs. The influence of chemistry is not modelled explicitly, but is accounted for by performing tests for different chemical environments, and/or concentrations.

Most of the test series are impressive and the results appear very logical and CT have succeeded in getting a good understanding of many of the important properties needed for the constitutive model describing the expansion of bentonite out into a fracture of a given width. Of course it is a challenge to perform tests at very high water contents, and probably, in spite of future extended testing, certain assumptions must be made for the extreme water contents. It should, however, not be so difficult to make reasonable assumptions and, in many cases, the possible variations in assumptions might not be crucial for the final modelling results.

This constitutive model models many of the important phenomena in a quantitative manner and the experimental back up is sound, even if much testing remains to be done. For example, it seems that all testing so far has been done for temperatures usually prevailing in the laboratory, which might be rather different from the temperatures expected in the final repository.

3.3.2 KTH model

The constitutive model presented by KTH is based on a chemical framework and testing of a more qualitative character (Neretnieks *et al.*, 2009). The Dynamic Force Balance Model is based on an assumption of force equilibrium amongst a number of forces including, buoyancy and gravity, van der Waals forces, repulsive double layer forces between particles, and friction against water. A thorough mathematical treatment, involving a number of simplifying assumptions, leads to a model that can describe a number of processes and be used to estimate the importance of the different phenomena. Surprisingly logical and reasonable results are obtained for many of the problems addressed.

Expected behaviour, based on geochemical theories and assumptions are analysed with the help of observations from different test set-ups. The tests give a good understanding of how the different processes involved might interact. Many of the CT test results are utilized in the KTH model and the tests are not duplicated. Again, it is important to bear in mind that the material behaviour, that of gels and sols are of utmost importance for the theories involved. Unfortunately testing of the material, as pointed out earlier, at these high water contents are extremely difficult to test quantitatively in the laboratory.

Perhaps most important is to understand the mechanisms and chemistry at the front where bentonite particles or molecules are torn off (eroded) and transported away by the flowing water.

The forces between the particles involved are extremely small and the energy necessary might be affected by temperature. This dimension is not addressed in detail and might need further attention

3.4 Spalling

Spalling caused by large differences in different principle stresses after the drilling of the deposition holes, and or worsened by temperature increase (thermal spalling), will increase not only the frequency of fractures but also the width of the fractures. This will in turn increase the amount of bentonite intruding into the fractures and thereby also possibly increase the rate of erosion, depending on the groundwater flow regime around the repository. This problem has been addressed by SKB, but insufficient information is yet presented in order to evaluate it.

3.5 Discussion of assumptions made

It is indeed difficult to understand the effect of every single different assumption made when building a constitutive model, not only because they might interact and be dependent on one another, but also because the effect might not be clear until a more comprehensive understanding is obtained. In spite of these difficulties or drawbacks, some assumptions are discussed separately below.

3.5.1 Geometry

The assumption of an idealized fracture with smooth walls and constant thickness is far from the geometry of a real fracture. However, the assumption is probably in most respects on the conservative side and unfavourable. A real fracture offers more opportunities for sedimentation and filter formation¸ very narrow parts might hinder or slow down expansion of the bentonite, discontinuities will decrease the effective porosity and tortuosity will increase the length of the flow paths, rough parts of the fracture walls might increase wall friction etc. Therefore, the assumption of an idealized fracture seems reasonable and on the safe side.

3.5.2 Geotechnical parameters

Comprehensive tests over the years have given a very good understanding of the strength and deformation properties of bentonite and the geotechnical parameters describing strength, swelling pressure and deformation of the material at densities when it can be regarded as a solid mass. As the material expands and transforms into a gel and sol it becomes more appropriate to describe flow properties for the material, rather than strength (see next section). The models used for bentonite are in line with what is usually done within the field of geotechnical engineering. Although more advanced models are readily available, the present analysis probably would not benefit from a more detailed or sophisticated description of the material behaviour and a more complex representation is thus not necessary.

However, wall friction or shear stresses exerted by the fracture wall on the material in the fracture has a great impact on the penetration depth of the bentonite. The CT model assumes a wall friction of 10 to 20 degrees, whereas the KTH model assumes that the wall friction can be neglected. This latter assumption leads to an expansion into the fracture approaching infinity, while the CT model results in intrusions of a few mm to a cm, depending on fracture width. It is obvious that further research and testing is necessary to increase the understanding of the different mechanisms involved. It is reasonable to assume that wall friction is a major factor hindering expansion for the bentonite in a solid state. To what extent it is so also for the gel or sol state is less well understood. Well-planned experiments could possibly improve the understanding of this issue.

3.5.3 Flow properties

As the water content of the bentonite increases it has been found that the material behaviour can be modelled using rather conventional models for flow instead of a stress-strain relation. A couple different models have been tested and it seems that a gradual change of the set of parameters can reasonably well describe the behaviour observed in the laboratory. A stress-strain relation is used in the CT model for a gel with a water/clay ratio less than 35. A power law is recommended for ratios from 35 to 70, and then, for ratios up to perhaps 500, the sol is best described as a Newtonian liquid. For even higher water/clay ratios, it can be regarded as water and assigned a viscosity.

Parameters for the different models have been determined for a couple of different materials and the tests have been made for a number of well defined chemical conditions. Further testing might facilitate a more general description of a model accounting for a variety of conditions.

3.5.4 Mechanism for erosion

There seems to be a consensus that, given that a fracture exists, the bentonite will expand and gradually transform from a highly compacted solid mass to a gel and a sol and that erosion in a fracture might occur when fresh water flows by tangentially. How extensive this expansion will be depends

strongly on the assumptions regarding wall friction and water flow rates. Theoretical speculations suggest that irrespective of the extent of the expansion no erosion will occur for the water flow velocities expected, as long the chemical conditions are such that colloidal suspensions of clay are not stable.

However, when water salinities decrease and conditions are such that stable colloidal suspensions can form, the gel becomes repulsive and material will expand into the flowing water and be carried away by the flowing water. The amount of material eroded in this way is dependent on the velocity of the flowing water and the speed at which the bentonite will be supplied at the sol/water front, as a result of expansion of the bentonite. Attempts have been made to model this expansion with FEM analysis and this results in bentonite losses of anywhere from a few kg to a 100 kg per 100 years for a 1 m wide fracture. These numbers are very preliminary and much more modelling needs to be done.

4. Buffer-groundwater interactions

Buffer erosion may take place in response to changing pore fluid compositions in bentonite, such as due to the infiltration of dilute groundwater during glacial periods. However, the pore fluid composition in compacted bentonite is chemically 'conditioned' by various processes, such as ion exchange, protonation-deprotonation reactions at clay edge sites, and by mineral hydrolysis. These reactions cause a strong buffering effect (*e.g.*, Savage *et al.*, 2010).

Moreover, there is considerable debate about the nature of porosity in compacted bentonite and the implications of this for the composition and evolution of pore fluid chemistry and for the transport of cations and anions. The debate focuses on two key questions:

- do different types of porosity exist, or can solute transport behaviour be explained by a single porosity model?, and
- what are the implications of different porosity models for buffer erosion?

Models of buffer erosion have to take into account controls on pore fluid evolution and be consistent with the theoretical understanding of the nature of porosity in compacted bentonite.

4.1 The nature of porosity in compacted bentonite

Intimately related to any model of bentonite erosion (as well as of other processes, such as re-saturation and swelling, evolution of pore fluid chemistry, etc.), is the understanding of the nature of porosity and the behaviour of fluids in close proximity to charged clay surfaces. Currently-available conceptual models for clay-pore fluid behaviour consist of either a system with different porosity types, or a system with a single porosity. Both concepts are discussed in more detail below.

4.1.1 Multiple porosity model

Many researchers view compacted bentonite as possessing different types of porosity (*e.g.* Kozaki *et al.*, 1998; Kozaki *et al.*, 2001; Bradbury and Baeyens, 2002; Bradbury and Baeyens, 2003; Kozaki *et al.*, 2005; Muurinen and Carlsson, 2007; Glaus *et al.*, 2007). The following types of porosity have been proposed (Figure 4.1.1_1).

- 'Total' porosity, which refers to the total volume of voidage without discrimination regarding location or type.

- ‘Interlamellar/interlayer’ water, which is located in the interlayer spaces of clay particles between the individual tetrahedral-octahedral-tetrahedral (TOT) sheets (Bradbury and Baeyens, 2003). This type of water is considered to be a few monolayers thick and, because of its more structured nature, is likely to have different properties from so-called ‘free’ water.

- ‘External’ water, which can be viewed as being of two types:
    - that which consists of water in electrical double layers on the surfaces of the clay particles (‘double layer water’); and
    - ‘free water’ (Bradbury and Baeyens, 2003) or ‘chloride’ porosity (Muurinen and Carlsson, 2007), which consists of water existing as interconnected thin films on the outside of clay stacks and also as films surrounding other minerals (*e.g.* quartz) in the bentonite.

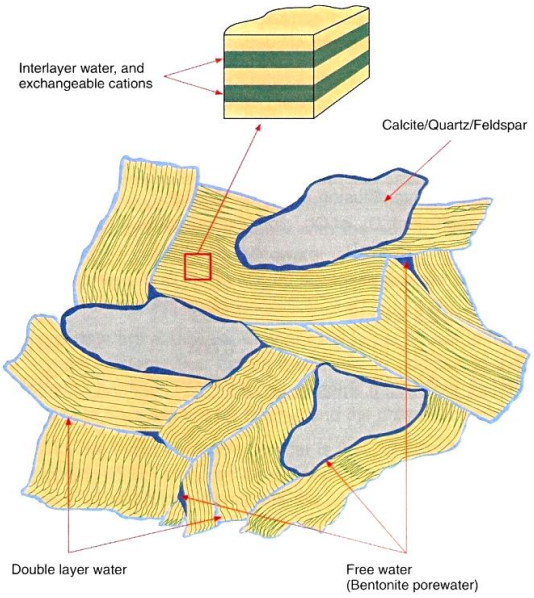

Figure 4.1.1_1. Schematic diagram of the nature of water in compacted bentonite. From Bradbury and Baeyens (2003).

The amounts of each porosity type vary with compaction density in bentonite according to Muurinen and Carlsson (Muurinen and Carlsson, 2007), with ‘free water’ or ‘chloride porosity’ being significantly less than the total porosity as compaction density increases.

In terms of transport, diffusion of cations is envisaged to take place both through the interlamellar porosity and the free porosity, whereas diffusion of chloride and other anions takes place solely though the free porosity (*e.g.* Glaus *et al.*, 2007). At high ionic strengths, diffusion of cations is thought to take place preferentially though the free porosity. This interpretation leads to an effective diffusion coefficient which varies according to ionic strength.

4.1.2 Single porosity model

An alternative conceptual model to that described above is offered by Karnland and co-workers (Karnland *et al.*, 2002; Birgersson and Karnland, 2009). The model is based on the assumption that a bentonite-pore fluid system consists of only one type of porosity. The pore fluid composition is controlled by ion equilibrium within the interlamellar pore space involving two basic processes:

- Donnan equilibrium, which reduces concentrations of external ions compared with external pore fluids; and

- cation exchange, which affects systems only with more than one type of cation.

Consequently, the clay-pore fluid system is envisaged to consist of clay particles acting as macro-ions, and the entire clay-water system may be viewed as a 'polyelectrolyte'.

Birgersson and Karnland (Birgersson and Karnland, 2009) argue that the acceptance of the existence of only one type of porosity in compacted bentonite obviates the need to describe two separate methods of describing anion and cation diffusion and, thus, their model brings a greater symmetry to the understanding of transport in compacted bentonite. Removing all but one type of pore structure greatly reduces the amount of model parameters to just one, the interlayer pore diffusivity (D_c). Furthermore, the single pore type model is not only consistent with, but also allows for accurate calculation of the swelling pressure under various physicochemical conditions (Karnland *et al.*, 2005; Birgersson *et al.*, 2008).

The findings of Birgersson and Karnland (Birgersson and Karnland, 2009) also have large implications for the conceptual view of pore water chemistry and, hence, the trigger for buffer erosion. Since in their model, the major part of the cations and anions reside in the interlayer pores, this volume is of crucial importance and cannot be ignored in characterising the bentonite pore water chemistry. This approach is, thus, in sharp contrast to the 'multiple porosity' model where pore fluid is considered to reside in the 'free water' porosity only.

4.2 Mass balances and key processes

Bentonite properties and pore fluid composition will depend upon its constituent minerals and its compaction density as well as:

- the proportion and type of montmorillonite;
- the types and amounts of trace minerals; and
- 'external factors' such as the salinity of saturating groundwater.

Pore fluid is chemically 'conditioned' within the bentonite by various processes:

- clay ion exchange (rapid);
- clay edge site protonation-deprotonation (rapid);
- dissolution of trace gypsum (rapid to slow);
- hydrolysis of clay and trace silicates (slow).

4.2.1 Mineralogical constituents

The reference composition for MX-80 bentonite (2000 kg m^{-3} saturated density) is shown in Table 4.2.1_1. This composition is calcite-free, so that gypsum is the principal solid source of readily available calcium ions in the bentonite. This composition contains 87 wt % Na-montmorillonite and up to 204 kg of non-clay minerals per cubic metre of bentonite.

Table 4.2.1_1 Composition of MX-80 bentonite at the reference dry density of 1570 kg m^{-3}. From Arcos *et al.* (Arcos *et al.*, 2008).

	wt %	**kg m^{-3}**
Montmorillonite	87.00	1365.90
Quartz	5.20	81.64
Feldspar (+ mica)	7.00	109.90
Pyrite	0.10	1.57
Gypsum	0.70	10.99
Total non-clay	13.00	204.10
Total solids	100.00	1570.00
Water	-	429.09
Solids + water	-	1999.09

4.2.2 Ion exchange

For the most part, cation exchange is the most important reaction governing pore fluid chemistry. Ion exchange is fast (effectively instantaneous) and can contribute 1024 chemical equivalents per cubic metre of bentonite (Table 4.2.2_1).

Table 4.2.2_1. Clay ion exchange reactions and exchange equivalents per 100 g and exchange equivalents per m^3 bentonite in MX-80 bentonite at reference density. From Arcos *et al.* (Arcos *et al.*, 2008).

Reaction	**Log *K***	**%**	**meq/100 g clay**	**Total eq m^{-3} bentonite**
$X^- + Na^+ = Nix$	0.00	72	54.0	738
$X^- + K^+ = KX$	0.60	2	1.5	20
$2X^- + Ca^+ = CaX_2$	0.41	18	13.5	184
$2X^- + Mg^+ = MgX_2$	0.34	8	6.0	82
Totals	**-**	**100**	**75.00**	**1024**

4.2.3 Clay protonation-deprotonation reactions

Clay protonation-deprotonation reactions on clay edge sites also offer instantaneous equilibration for pH buffering, but offer approximately a factor of 20 fewer sites than for conventional cation exchange (Table 4.2.3_1).

Table 4.2.3_1. Clay edge site protonation-deprotonation reactions and amounts per kg clay and per m^3 bentonite. From Arcos *et al.* (Arcos *et al.*, 2008).

Edge site protonation-deprotonation	Log *K*	Mol kg^{-1} clay	Mol m^{-3} bentonite
$S^1OH + H^+ = S^1OH_2^+$; $S^1OH = S^1O^- + H^+$	4.50; -7.90	0.04	27.5
$S^2OH + H^+ = S^2OH_2^+$; $S^2OH = S^2O^- + H^+$	6.00; -10.50	0.04	27.5
Totals	**-**	**0.08**	**55.0**

4.2.4 Trace mineral reactions

Abundances and hydrolysis reactions for trace minerals in bentonite are shown in Table 4.2.4_1. SKB's near-field simulations for SR-Can show that (equilibrium) gypsum dissolution in granite groundwater removes 50% of the initial amount of gypsum after 1000 years with complete removal after 20000 years (Arcos *et al.*, 2008). Treating this reaction more realistically (kinetically) would increase gypsum's persistence in the near-field and should be considered in future modelling calculations to evaluate if gypsum could buffer Ca^{2+} concentrations to values above the CCC, and, if so, for how long.

Table 4.2.4_1. Amounts of trace minerals and hydrolysis reactions for the MX-80 composition at reference density. From Arcos *et al.* (Arcos *et al.*, 2008).

Mineral	kg m^{-3} bentonite	Hydrolysis reaction	Log *K*
Quartz	82	$SiO_2 = SiO_{2(a)}$	-3.99
Feldspar	110	$NaAlSi_3O_8 + 4H^+ = Na^+ + Al^{3+} + 3SiO_{2(a)} + 2H_2O$	2.76
Pyrite	1.6	$FeS_2 + H_2O = Fe^{2+} + 2H^+ + 1.75HS^- + 0.25SO_4^{2-}$	-24.65
Gypsum	11	$CaSO_4.2H_2O = Ca^{2+} + SO_4^{2-} + 2H_2O$	-4.85

4.2.5 Kinetics of clay hydrolysis reactions

Compared with ion exchange reactions, clay hydrolysis is slow, with a rate constant in the order of 10^{-14} mol m^{-2} s^{-1} at neutral pH (Sato *et al.*, 2004). This translates to 4 10^{-7} mol s^{-1} m^{-3} bentonite. Despite this slow rate, Savage *et al.* (Savage *et al.*, 2010) have shown that hydrolysis reactions can be important in buffering pore fluid pH in the long-term (>10^3 years) and should be considered in models of buffer erosion.

4.3 Geochemical constraints on gel/sol stability

Birgersson *et al.* (2008) use mass-action and mass-balance constraints on ion-exchange reactions to interpret stability relations among montmorillonite sols, gels and flocs. Flocs are predicted to be stable when the Ca/Na ratio in the clay > 90/10 and aqueous Na^+ concentrations are low. Cohesive gels are predicted to be stable when the ionic strength > 25 mM and the Ca/Na ratio in the clay < 90/10. Sols are predicted to be stable under these conditions when the ionic strength < 25 mM.

The predicted stability field of bentonite clay sols is quite small and occurs over a range of very low Na^+ and Ca^{2+} concentrations[8]. This range may be compatible with the compositions of glacial meltwaters, however, which suggests that even essentially pure Ca-montmorillonites would be susceptible to chemical erosion should they be used as buffer materials in a KBS-3 repository. Any strategy to mitigate the potential effects of chemical erosion by choosing bentonites composed of Ca-montmorillonite rather than mixed Na/Ca- or Na-montmorillonite will likely also have to contend with the possibility that ion-exchange reactions, occurring over time scales of hundreds-of-thousands of years, could significantly alter these Ca-montmorillonites to more sodic forms.

[8] Recent experiments suggest that this field is even smaller than predicted (Birgersson et al., 2008).

5. Potential for Filtration to Mitigate Buffer Erosion

5.1 Introduction

SKB has carried out an investigation of filtration as a mitigating process to sustained erosion of the bentonite buffer barrier of the KBS-3 concept for geological disposal of spent nuclear fuel. The basic concept investigated by SKB envisioned extrusion of bentonites into intersecting fractures, followed by loss of colloidal smectite under certain environmental conditions (see Sections 2.1 and 2.2). SKB researchers speculated that accessory phases within the bentonites, such as quartz, feldspar, etc., might be left behind after removal of smectite colloids and might eventually accumulate to form a 'filter cake'. Depending on the extent, properties, and durability of such a filter cake, further removal of smectite colloids from the buffer into the fracture might be impeded or prevented, thereby providing an inherent mechanism to minimize or prevent sustained buffer erosion.

In its studies on this filtration process, SKB researchers developed theoretical models for guiding the design and analysis of experiments. Independent laboratory tests were made to examine the effectiveness of pre-fabricated filter cakes in filtering of colloidal-sized particles as surrogates of smectite colloids (Birgersson *et al.*, 2009; Neretnieks *et al.*, 2009; Richards 2010).

A 'decision-tree' approach is taken here to evaluate the results and implications of these SKB-sponsored studies. In a 'decision-tree' evaluation, a series of questions is posed regarding the postulated behavior or scenario, in this case the mitigation of buffer erosion by formation of a filter cake composed of accessory minerals. The questions are stated in such a way that all questions must be answered 'yes' for the postulated behavior or scenario to be valid. If even one question is answered 'no', however, then the postulated behavior or scenario is rejected as being invalid (or unsupported).

Figure 5.1_1 shows the 'decision-tree' set of questions formulated to evaluate the postulated mitigation of buffer erosion by filter cake formation. In the following sections, each of these questions is evaluated in turn. Based on the individual evaluations of each question, a final section presents an expert judgment regarding the validity and reliability of relying on formation of a filter cake to mitigate sustained buffer erosion.

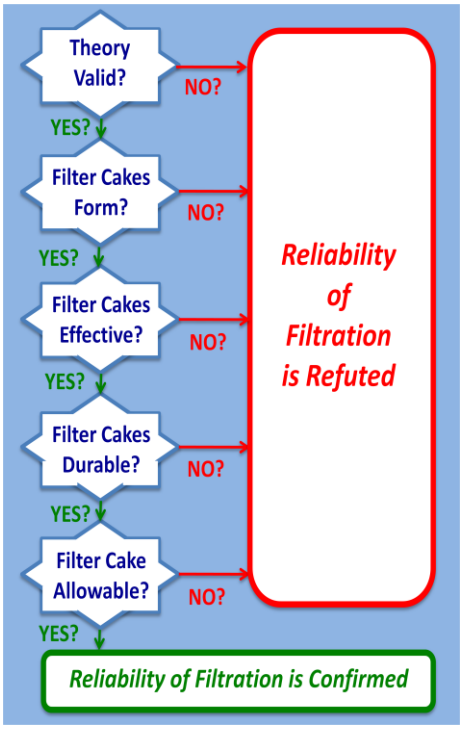

Figure 5.1_1. Decision-tree format used to evaluate the postulated mitigation of sustained buffer erosion arising from formation of accessory-mineral filter cakes.

5.2 Is filtration theory valid?

Birgersson *et al.* (2009), Neretnieks *et al.* (2009) and Richards (2010) each describe theoretical models of the formation and effectiveness of filtration beds. Several alternative filtration theories have been developed and tested in industrial contexts. Richards (2010) notes that "*DLVO and the convective-diffusion equation predicts the right magnitude of colloid removal efficiency when no energy barrier exists; however, when energy barriers exist, discrepancy is large*." Based on his evaluation of various filtration models, Richards (2010) adopts the packed-bed approximation as an initial basis for interpreting his subsequent experimental results.

The limitations in applying any of the existing industrial-based filtration theories to the buffer-erosion scenario are discussed by Birgersson *et al.* (2009), Neretnieks *et al.* (2009) and Richards (2010). These limitations include:

- the absence of consideration of the effect of electrically charged surfaces and associated forces;
- the presence of a fluid phase in addition to assumed 'surfaces' of filter and particle;

- irregular shape, size and distribution of solids in realistic filter cakes;
- change in filter porosity over time due to 'clogging'; and
- the need to develop several empirical ('fitting') factors, meaning that there is a very limited ability to extrapolate laboratory results from one set of environmental conditions to a different set of environmental conditions (this might include the inability to use data from one type of bentonite for another).

In conclusion, the answer to the question "*Is filtration theory valid?* is a qualified 'yes'. Such theories are constrained largely by empirical observations, cannot easily be extrapolated to new situations and have limited predictability. There are many limitations that need to be considered when such theories are used to quantify filtration efficiency.

5.3 Do filter cakes form?

The formation of a filter-cake under repository conditions, as buffer extrudes and erodes into fractures, seems to be simply assumed in all the SKB-sponsored studies noted above. This assumption is likely based on the observation that bentonite clays do contain a proportion of such accessory phases and that preferential loss of clay colloids, would leave behind a collection of such accessory minerals, *e.g.*, quartz, feldspar, pyrite, oxides, organics(?) and possibly other residual phases. There is some limited photographic evidence of a dark ring of such residual material after smectite has been removed (Richards 2010). However, such a collection of residual particles has not been shown to even approximate the uniform packed filter-cakes, or metal filters used in the experiments of Richards (2010) and Birgersson *et al.* (2009), respectively.

It is unfortunate that the development (and properties) of the postulated filter cakes have not been addressed by SKB. These data are absolutely critical to justifying and supporting SKB's postulated filter cake scenario. There has been no post-experiment analysis to confirm the development, or measure the properties, of a filter-cake resulting from buffer erosion. Birgersson *et al.* (2009) simulated the development of a residual phase (it cannot be confidently called a 'filter cake') but, to our knowledge, no post-test analysis of the residual phase was made. The possible occurrence of natural analogues of such filter cake formation was identified as a potentially useful area for confirmatory study, but SKB has not provided a clear demonstration that effective filter cakes do actually form as a result of bentonite erosion.

The final evaluation is that the question "*Do filter cakes form?*" is a qualified 'no' at the present time. The uniform packed beds and metal-filter analogues used in the SKB-sponsored studies noted above do not provide convincing evidence that filter cakes could form in a KBS-3 repository.

5.4 Are filter cakes effective?

Richards (2010) used a pressure-induced flow of a suspension of 200-nm diameter smectite particles through pre-formed filter cakes of Na-MX80 or additives to evaluate filtration effectiveness. He used natural accessory minerals having a diameter range of 5-10 μm, and also examined filtration by filter cakes composed of different ratios of industrial materials, apparently as possible additives to a buffer to further mitigate buffer erosion. Richards (2008) conducted sensitivity studies using different thicknesses of filter cakes and filtration at different pH values.

There are several concerns regarding the Richards (2010) test results and interpretations of filtration effectiveness. First, up to 40% of the original bentonite buffer material was lost during the preparation of filter cakes. The author did not address if and how such losses occurred, and what might be the impact on the representativeness of subsequent tests relative to actual repository conditions. Second, the irregularity of the mineral grains versus the assumed spherical nature of filter particles in the applied theory was mentioned, but was not addressed or bounded in the interpretation of results. Third, it is not clear if pressure-induced flow of clay colloids through packed bed filters is a reasonable representation of actual filtration that might occur under repository conditions. There was no consideration if induced flow, or even long-term colloid stability, might unrealistically enhance measured filtration efficiency.

Birgersson *et al.* (2009) conducted experiments on the diffusion of clay colloids, formed within various buffer compositions, through pre-formed filters of various sizes and thicknesses into deionized water flowing past the filters at a rate of 1 ml min^{-1}. Use of diffusive transport, rather than advective flow as in Richards (2010), was judged by Birgersson *et al.* (2009) to be a strong advantage in attempting to simulate actual repository conditions. MX-80, homoionic Na- and Ca-montmorillonites, kaolin and diatom additives, and >2 μm accessory minerals from MX-80 were used to form the filter cakes. The filtration effectiveness was determined by measuring both the swelling pressure drop in a buffer sample, and changes in the turbidity of the circulating water over time (see Section 2.3.3 and Figure 2.3.3_2).

The following combinations of filter cake material and pore size were found by Birgersson *et al.* (2009) to stop colloid release by diffusion into the flowing water:

- homoionic calcium clay with pore size < 100 μm;
- homoionic sodium clay with pore size < 0.5 μm;
- homoionic sodium clay and a compacted 2 mm-thick layer of either kaolinite or diatomite;

Birgersson *et al.* (2009) suggested that other filter materials can be expected to have similar sealing properties as kaolinite provided they have a similar grain-size distribution, but the basis for this statement is unclear.

As noted earlier, there was a missed opportunity by Birgersson *et al.* (2009) to examine and confirm the development and structure of a filter cake of accessory minerals formed from buffer erosion of MX-80 during their tests.

In summary, the answer to the question "*Are filter cakes effective in mitigating the loss of clay colloids*?" is judged to be 'maybe'. This answer is equivocal because it has been assumed that the pre-fabricated filters used in the Richards (2010) and Birgersson *et al.* (2009) tests are representative of filter cakes that might form under actual repository conditions. As noted in the previous section, this assumption is, at this point, unsubstantiated, so that the effectiveness of filtration shown in the SKB-sponsored tests may, or may not, be reasonable representations of actual buffer behavior in a repository.

SKB does not seem to have addressed issues associated with the effects of spatially and temporally variable groundwater flows on the overall potential ability of a system of filter cakes in a repository setting to limit bentonite erosion. Indeed, in its latest safety assessment, SKB has not relied on the formation or effectiveness of filter cakes in the repository system, and so at this point SKB has not put forward a conceptual model for the formation of filter cakes in fractures surrounding the disposed wastes on a relevant repository scale.

5.5 Do filter cakes persist?

This question does not seem to have been explicitly considered in any of the SKB-sponsored studies, yet it is important because the formation and long-term stability of filter cakes could affect various safety functions of the buffer. There are numerous ways in which a filter cake, if formed with sufficient properties to effectively filter clay colloids, might be compromised over time under reasonable and foreseeable repository conditions. Earth tremors might be sufficient to cause the mechanical breakdown of a filter cake. Slight shearing or expansion/ contraction of a fracture (possibly due to glacial loading and unloading) might also mechanically breakdown a filter cake. Would possible changes in flow rate or direction also affect filter cake durability? It might be possible to locate and evaluate suitable natural analogues that could be used to help to address this question.

The answer to this question "*Do 'filter cakes' persist over relevant repository timescales and future events?"* is also 'maybe', or perhaps would be better expressed as 'unproven' since there are no data or analyses reported by SKB researchers on this topic. Of course it must be stressed that an equivocal answer to any of the questions in the decision tree (Figure 5.1_1) must be treated from a regulatory perspective as being a 'no'. It is up to the implementer to support and defend any 'yes' answer to these questions.

5.6 Can safety functions be assigned to a degraded barrier?

Filter cakes are not a formal part of the KBS-3 design concept; they have been speculated by some researchers to form from the degradation of the

initial bentonite buffer. It is not clear how much performance and safety reliance can be placed on the properties of a degraded buffer and formation of a filter cake. This is another question that has not been addressed in the SKB-sponsored studies on filter cakes and filtration.

There can be no pre-closure quality assurance of the properties of such a degraded barrier, and the range of possible filter cake properties as formed in the far future would seem to be quite uncertain. If a safety function (*e.g.*, 'mitigate sustained buffer erosion') were to be assigned to a filter cake composed of accessory minerals, it would seem that an extremely large amount of data, alternative conceptual models, alternative scenarios, and variable environmental conditions would need to be evaluated and confirmed. There may be ways to approach and achieve such strict confirmation, but there does not seem to be an acknowledgment or consideration of the need for this effort in any of the SKB-sponsored studies to date. Because this is a regulatory topic, no attempt is made to provide an answer to this question.

6. Conclusions

This section provides a summary of conclusions derived from the discussions in Sections 2 – 5.

6.1 Chemical aspects of buffer erosion

Neretnieks *et al.* (2009) developed a model of buffer erosion that is based on a force-balance model and a viscosity model of colloid-water interactions. The force-balance model considers the van der Waals force, the diffuse double-layer force, the thermal force giving rise to Brownian motion, friction forces between colloidal particles, and the gravitational force. The viscosity model accounts for the influence of the double layer force on particle size, and for viscous interactions among the particles as a function of particle density.

The buffer erosion model was evaluated by Neretnieks *et al.* (2009) for idealized systems of pure Na-montmorillonite colloids in simple NaCl solutions. Neretnieks *et al.* (2009) assume such systems are conservative because montmorillonites containing predominantly Ca^{2+} rather than Na^{+} on exchange sites tend to form stable gels as a result of an additional attractive force between particles arising from ion-ion correlations. The buffer-erosion model predicts a strong dependence of colloid formation and expansion in a fracture on the concentrations of counterions in the double layer and on the particle concentration of the gel or sol.

DLVO theory was adopted by Neretnieks *et al.* (2009) to handle the repulsive double-layer force and attractive van der Waals force between colloidal particles. There is a general consensus that the conceptual basis of DLVO theory is substantially correct, but that it is also deficient in some important respects. In general, the deficiencies arise for two reasons: oversimplification of the properties of real colloids, and omission of non-DLVO forces that can be important under certain circumstances. For example, montmorillonite colloids carry a net negative charge on faces oriented parallel to the dominant tetrahedral-octahedral-tetrahedral layering, and, depending on pH, net positive or negative charges on edges that are oriented normal to this layering. A given montmorillonite particle can thus have different double-layer structures associated with its faces and edges. DLVO theory also does not account for the effects of specific adsorption on colloid stability. Electrolytes in real clay colloidal systems may form covalent complexes with functional groups at the particle's surface. Such complexes alter the surface charge and surface potential, and thereby affect colloid stability. H^{+} and OH^{-} are particularly important potential-determining ions because they react with the surface sites of clay minerals. The colloidal stability of these minerals is thus pH-dependent, but this dependency is not accounted for in DLVO models. These potential deficiencies and limitations in DLVO theory raise questions regarding the validity of the assertion by Neretnieks *et al.* (2009) that their buffer erosion model is conservative because it considers only pure Na-montmorillonite colloids in simple NaCl solutions.

The results of SKB's R&D program indicate that buffer erosion may occur if the clay buffer is exposed to flowing water having low concentrations of calcium (or other divalent/trivalent cations), and if NaCl concentrations do not exceed 25mM (*e.g.*, Neretnieks *et al.*, 2009; Birgersson *et al.*, 2009). The observation that clays swell to a finite concentration only when the Ca/Na ratio in the clay exceeds 9 is in quantitative accordance with predictions based on the primitive model. The model used to analyze ion exchange between the bulk aqueous solution and clay (Birgersson *et al.*, 2009) is rather approximate because it does not account for differences in the concentrations of exchangeable cations in interlayer regions of the clay particles and the bulk solution.

The variability in properties of the clay minerals in bentonite is a complication that has received relatively little attention in SKB's R&D program. There will inevitably be some variation in the properties of clays minerals that are extracted from a specific source quarry over periods of decades or longer. More subtle effects could arise from microscopic variations in the properties of clay particles within a given sample. For example, there is little information available characterizing the variance in charge density relative to its mean value in a macroscopic sample. Some of the experimental findings reported in SKB's R&D program might be due to such heterogeneities in the properties of clay particles.

SKB and others have conducted a range of experiments that have investigated some areas of the bentonite erosion issue. Some of these experiments are of a problem-scoping nature and represent the early stages of research into bentonite erosion. Some of the experiments go further, are relatively more refined, better focussed and constrained but, in total, the range of experiments conducted to date is limited, and only some areas of the problem have been addressed. For example, further work would be needed to properly understand the role of dissolved Ca in preventing erosion of Na-rich clays. Given the small number of experiments performed, it is not yet possible to comment on the reproducibility of the findings.

In addition, some of the experiments that have been conducted have highlighted processes (*e.g.*, the effect of dispersed bentonite on water flow) that are not accounted for in the current conceptual models. SKB's conceptual model is a significant simplification compared to the real repository situation.

There are also several questions over how relevant the experiments are to the repository system. For example, real fractures in the repository environment will be rough, will have various orientations, intersections and asperities, and on average may be approximately ten times narrower than considered in the experiments. This issue of physical scale is also potentially important as none of the experiments has been conducted over length scales greater than a few centimetres. Clay penetration distances into fractures could be smaller than calculated in some of the simulations discussed by Birgersson *et al.* (2009), but there is no real experimental evidence to confirm this. There is no convincing experimental evidence that the accessory minerals in com-

mercial bentonite will form effective filters, as postulated by Neretnieks *et al.* (2009).

SKB has made important progress in developing an understanding of chemical aspects of the bentonite erosion issue. Additional research and assessment would likely lead to improvements and refinements in this understanding. It is not clear whether the buffer erosion model developed by Neretnieks *et al.* (2009) is adequately conservative in the sense that predictions made using the model establish a defensible upper bound on the erosion rate over a plausible range of near-field conditions.

6.2 Physical aspects of buffer erosion

SKB has presented two different approaches for modelling physical aspects of buffer erosion. One approach is based entirely on classical material behaviour and comprehensive experiments in the laboratory. The other approach is based on a more theoretical force-balance analysis, where laboratory tests are used to verify the theories in a more qualitative way. The behaviour of the solid material is well understood and the research in this area can be regarded as mature. When it comes to gels and sols more testing is necessary to understand and demonstrate the functionality of the different constitutive models.

The rate of expansion of the solid material, as well as the rate at which the bentonite might be fed to the front where erosion occurs, needs to be further investigated. The presence or absence of wall friction is an issue that should also be addressed in future studies.

6.3 Buffer-groundwater interactions

There is considerable debate about the nature of porosity in compacted bentonite and the implications of this for transport of cations and anions. It is unclear whether different types of porosity must be considered, or, alternatively, whether solute transport behaviour can be explained using a single porosity model. A single porosity model appears to be consistent with swelling pressure data. Models of buffer erosion should investigate both concepts to evaluate the most relevant framework.

Bentonite pore fluid is chemically ‘conditioned’ within the bentonite by various processes and relevant mass balances:

- clay ion exchange (rapid);
- clay edge site protonation-deprotonation (rapid);
- dissolution of trace gypsum (occurring at rates between those of ion exchange and aluminosilicate mineral hydrolysis);
- hydrolysis of clay and trace silicates (slow).

Any plausible model of erosion has to be consistent with these factors.

Mass-action and mass-balance constraints on ion-exchange reactions provide a useful framework for interpreting stability relations among montmorillo-

nite sols, gels and flocs. Birgersson *et al.* (2009) have used such an approach to determine that the stability field of bentonite clay sols is quite small and occurs over a range of very low Na^+ and Ca^{2+} concentrations. This range in concentrations may be compatible with the compositions of glacial melt-waters.

6.4 Filtration

Using a decision-tree approach, several basic questions have been posed regarding the evidence presented in SKB-sponsored reports on the potential mitigation of long-term buffer erosion by the formation of filter cakes. While the theoretical and filtration efficiency questions can be reasonably answered 'yes' at this time, there is no convincing evidence or even a conceptual model for the formation of an effective system of filters at a relevant scale in a repository system. The important question on the properties of 'as-formed' filter cakes under repository conditions has not been sufficiently addressed, and the long-term durability of any filter cake that might form has also not been considered sufficiently.

7. Summary of key issues

A number of safety-relevant issues emerge from the overview of concepts regarding buffer erosion given in Sections 2 to 5. These issues are summarized below together with recommendations to help resolve them.

7.1 Erosion rates and mass-loss tolerances

Buffer erosion entails consideration of two key concepts: (1) the erosion rate, and (2) the amount of buffer mass loss that can be tolerated before safety functions are adversely impacted. Most work to date has focussed on the first of these concepts.

The second concept deserves further study. SKB's assessment (SKB, 2006a) that 1200 kg of bentonite can be lost from a deposition hole is based on an analysis that that is subject to considerable uncertainty regarding the nature of friction forces within the buffer and at the buffer-rock interface (Börgesson and Hernelind, 2006). At issue is the question whether the buffer would homogenize quickly and completely throughout the deposition hole following a loss of mass by erosion, or whether the effects of mass loss would be localized in the near vicinity of the fracture intersection with the buffer for long periods of time. SSM should carry out an independent evaluation of these uncertainties in order to help determine whether SKB's criteria for unacceptable mass losses of the buffer are credible and conservatively bounding.

7.2 Impacts on all relevant safety function indicators

The SR-Can safety assessment considered buffer erosion only in terms of the effects of a loss of density on the swelling pressure (p_{swell}) and associated effects on the buffer's safety function to limit advective transport. It is worth noting, however, that p_{swell} also relates to other safety functions of this barrier (*e.g.*, Figure 7.2_1). These functions include the ability of the buffer to effectively eliminate microbial activity, prevent canister sinking, and to allow gases produced within a potentially damaged canister to migrate out of the buffer without causing irreversible damage to the buffer's physical properties. Similarly, the buffer's density controls the safety function to ensure protection of the canister from the effects of rock shear, and two safety function indicators: hydraulic and thermal conductivity.

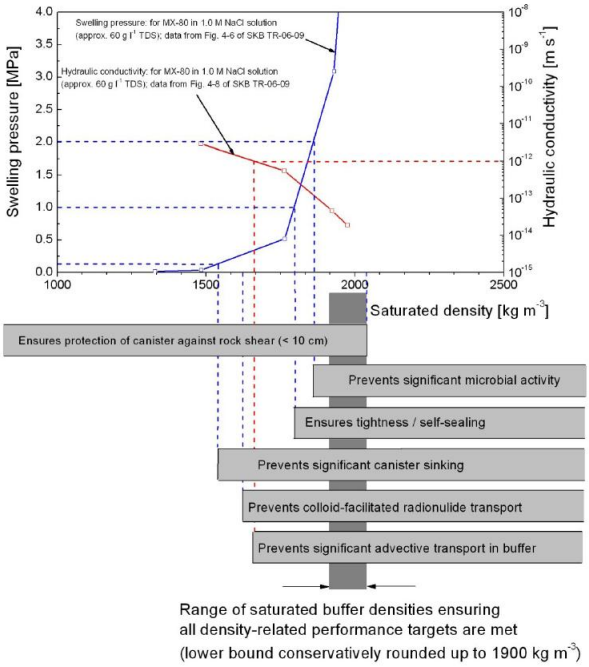

Figure 7.2_1. Schematic illustration of the effects of buffer saturated density on the swelling pressure, hydraulic conductivity, and related safety functions (Posiva, 2010).

Figure 7.2_1 indicates that mass losses leading to a reduction in saturated density would impact two safety functions (prevent significant microbial activity and ensure tightness/self-sealing) before they would impact the threshold for significant advective transport to occur. Only the latter safety function was considered in SR-Can, however. It is unclear if, and if so how, SKB will treat these other impacts on safety functions in SR-Site. It is recommended that these effects be further considered by SSM.

7.3 Force-balance and viscosity models

The force-balance model of Neretnieks *et al.* (2009) uses a DLVO-based representation of attractive and double-layer forces applied to an idealized system of pure Na-montmorillonite in a simple NaCl electrolyte solution. This representation is claimed to be conservative because repulsive forces favouring the formation of montmorillonite colloids should be maximized under these conditions in accordance with the Shulze-Hardy rule (Section 2.1.3).

As noted in Sections 2.1.4, 2.2.2 and 2.2.6, there is a general consensus that the conceptual basis of DLVO theory is substantially correct, but that the theory is also deficient in some important respects. This raises the question whether the claimed conservatism in the force-balance model is valid when these deficiencies are taken into account. Is it possible, for example, that conditions favouring the formation and stability of montmorillonite colloids (thus potentially enhancing the buffer erosion rate) are pH dependent? This

and other questions should be considered in relation to acknowledged deficiencies in DLVO theory (Section 2.1.4).

An empirical expression can be used to relate the relative viscosities of bentonite gels/sols to the volume fraction of the colloidal particles and to the ionic composition of the aqueous phase (Moreno *et al.*, 2009; Neretnieks *et al.*, 2009). The expression is constrained by experimental measurements of relative viscosities and particle volume fractions over a range of clay types and solution chemistry. It is not clear whether the expression is appropriate for conditions that lie outside this experimental range. The experimental conditions should be compared to those that are expected to be relevant to the near field of a KBS-3 repository at Forsmark.

7.4 Geochemical constraints on gel/sol stability

Construction of diagrams depicting the relative stabilities of montmorillonite gels and sols in terms of environmental variables such as the total analytical concentrations of Na^+ and Ca^{2+} is potentially very useful because conditions favouring sol stability are those for which the buffer is most susceptible to erosion (Section 4.3). Such diagrams are based in part on mass-action (*i.e.*, ion-exchange) constraints. Donnan equilibrium must also be invoked in order to relate the chemistry of solutions in the interlayer spaces between clay particles to the chemistry of an interconnected external reservoir represented by larger fluid-filled voids in the buffer and/or groundwater in the host rock.

As noted in Sections 4.1 and 2.2.4, there appear to be fundamental uncertainties regarding the nature of porosity in highly compacted clays, and ion-exchange models applied to such systems may be rather approximate. An evaluation of alternative models of the buffer-groundwater system based on different assumptions regarding the nature of porosity in the buffer and ion-exchange mechanisms could be used to gain a better understanding of how gel/sol stability relations can be interpreted in terms of groundwater chemistry and other environmental variables. The nature of porosity, and consequently pore water chemistry, in highly compacted clays is currently a subject of considerable debate in international nuclear-waste management programs.

7.5 Characteristics of glacial meltwaters

In SKB's models of buffer erosion glacial meltwaters are considered only in terms of the CCC for Ca^{2+} or the total number of equivalents of positive charge per unit volume of solution. An analysis of a pore water sample from the Grimsel test site in Switzerland is assumed to be representative of glacial meltwaters in general. SKB's participation in the Greenland Analogue Project (GAP), whose objectives include the development of a better understanding of the chemical characteristics of glacial meltwaters , may provide a basis for assessing whether this assumption is justified.

It is already known, however, that glacial meltwaters are not simple electrolyte solutions. A recent survey of the chemistry of such solutions indicates that they are indeed dilute solutions, but that cation and anion concentrations

can be quite variable (Brown, 2002). It is also important to distinguish between the total analytical concentrations of these ions and the chemical activities of individual aqueous species [*e.g.*, uncomplexed Ca^{2+}, $CaHCO_3^+$, $CaCO_3(aq)$, etc.]. There is also some evidence to suggest that such solutions would tend to promote ion-exchange reactions favouring the formation of montmorillonites having Ca^{2+} as the dominant cation occupying exchange positions. This is potentially important because ion-ion correlations favouring strong attraction between clay colloidal particles, thus tending to inhibit buffer erosion, are known to be important when Ca^{2+} constitutes more than 90% of the exchangeable cations. The process is, however, complicated by mass balance considerations, i. e., how much Ca^{2+} can be supplied from the glacial meltwater to the system during a certain period of time so that the bentonite can become cation-exchanged to Ca-bentonite. Transport and chemical processes controlling the chemical evolution of glacial meltwaters as they migrate from the surface toward the repository and interact with the host rock have received relatively little consideration in studies of buffer erosion. It is noteworthy in this regard that all of SKB's experiments on bentonite erosion to date have been conducted under oxidizing conditions with atmospheric levels of $O_2(g)$ and $CO_2(g)$. These conditions are unlikely to be characteristic of glacial meltwaters that evolve chemically as they migrate to repository depths.

Given these observations, it is recommended that SSM should further consider the chemistry and likely chemical evolution of glacial meltwaters in order to strengthen the scientific basis of SSM's independent assessments of whether buffer erosion could adversely impact repository safety.

7.6 Natural and anthropogenic analogues

Natural analogues have received relatively little consideration in studies of buffer erosion. Puura (2010) notes that although there are examples in which natural bentonites have been exposed to infiltrating meteoric waters, the relevance of observations from these systems to the issue of buffer erosion is questionable. Although this observation may be valid for the systems considered, it does not necessarily mean that there is little to be learned from other observations of the behaviour of clay minerals and clay colloids in natural systems that have been subjected to the effects of glaciation, or to perturbations in the natural environment resulting from human activities.

For example, clay minerals, including montmorillonites and other smectites, are common alteration products of water-rock interactions. They typically coat the surfaces of, or fill, fractures in crystalline rocks, and are thus analogous in this respect to scenarios that are believed to be relevant to buffer erosion. It is possible that these clay minerals would be susceptible to the effects of colloid formation and transport if glacial meltwaters migrated through the fractures during the past 100,000 years, and possibly also during earlier glacial cycles. The evidence for such clay erosion might be revealed by a systematic study of the relative abundances of clay minerals in fractures in the relatively near-surface of crystalline rocks that are known to have been exposed to the downward migration of glacial meltwaters over the past 100,000 years or longer. The extensive mineralogical characterization of

drillcore samples obtained in geoscientific investigations in Sweden and Finland could provide a solid foundation for such a study.

Insights regarding buffer erosion might also come from experiences gained in reservoir-engineering studies of producing oil/gas fields. It has been observed that significant reservoir damage (*i.e.*, permeability reduction) can occur in such systems when low-salinity groundwater is allowed to enter the reservoir (*e.g.*, Kia *et al.*, 1987). The damage is believed to occur when clay minerals in the reservoir are dispersed as colloids as a result of contact with the dilute groundwaters. The colloids are transported in the groundwater until they encounter local pore constrictions along the flow path. They are then deposited in these constrictions (presumably by gravitational and friction forces), and this results in an overall reduction in reservoir permeability. These processes are analogous to those that could occur during buffer erosion, which suggests that any clay lost from the buffer might tend to clog nearby fractures, thereby reducing groundwater flow rates in the vicinity of the deposition holes.

8. References

Abend, S. and Lagaly, G. 2000. Sol-gel transitions of sodium montmorillonite dispersions. *Applied Clay Science*, 16, 201-227.

Adamson, A. W. 1967. *Physical chemistry of surfaces, 2nd ed*. Interscience Publ., John Wiley & Sons, New York.

Arcos, D., Grandia, F., Domènech, C., Fernández, A. M., Villar, M. V., Muurinen, A., Carlsson, T., Sellin, P. and Hernan, P. 2008. Long-term geochemical evolution of the near field repository: Insights from reactive transport modelling and experimental evidences. *Journal of Contaminant Hydrology*, 102**,** 196-209.

Bennett, D.G., Crawford, M.B., Wickham, S.M. and Kessler, J. 1998. Multiphase-flow and colloid transport in total system performance assessment. In: Proc. Eighth Annual Int. High Level Radioactive Waste Management Conf. (Las Vegas, 11 - 14 May 1998), American Nuclear Society, La Grange Park, IL and American Society of Civil Engineers, New York, NY.

Birgersson, M. and Karnland, O. 2009. Ion equilibrium between montmorillonite interlayer space and an external solution. *Geochimica et Cosmochimica Acta*, 73**,** 1908-1923.

Birgersson, M., Karnland, O. and Nilsson, U. 2008. Freezing in saturated bentonite – A thermodynamic approach. *Physics and Chemistry of the Earth*, 33**,** S527-S530.

Birgersson, M., Börgesson, L., Hedström, M., Karnland, O., Nilsson, U. 2009. Bentonite erosion. SKB TR-09-34, Swedish Nuclear Fuel and Waste Management Co., Stockholm, Sweden.

Börgesson, L. and Hernelind, J. 2006. Consequences of loss or missing bentonite in a deposition hole: A theoretical study. SKB TR-06-13, Swedish Nuclear Fuel and Waste Management Co., Stockholm, Sweden.

Boström, M., Williams, D. R. M. and Ninham, B. W. 2001. Specific ion effects: Why DLVO theory fails for biology and colloid systems. *Phys. Rev. Lett.* (online), 87 (16), 168103, 4 pages.

Bradbury, M. H. and Baeyens, B. 2002. Porewater chemistry in compacted re-saturated MX-bentonite. Physicochemical characterisation and geochemical modelling. PSI Report 02-10, Paul Scherrer Institute, Villigen, Switzerland.

Bradbury, M. H. and Baeyens, B. 2003. Porewater chemistry in compacted re-saturated MX-80 bentonite. *Journal of Contaminant Hydrology*, 61**,** 329-338.

Brown, G. H. 2002. Glacial meltwater hydrochemistry. *Applied Geochemistry*, 17, 855-883.

Comsol. 2004. Femlab user's guide, version 3.1. The Comsol Co., Stockholm, Sweden.

Comsol Multiphysics. 2009. The Comsol Co., Stockholm, Sweden.

Derjaguin, B. V. and Landau, L. 1941. Theory of the stability of strongly charged lyophobic sols and of the adhesion of strongly charged particles in solutions of electrolytes. *Acta Phys. Chem.*, 14, 633.

Engström, S. and Wennerström, H. 1978. Ion condensation on planar surfaces. A solution of the Poisson-Boltzmann equation for two parallel charged plates. *Journal of Physical Chemistry*, 82, 2711-2714.

Evans, D. F. and Wennerström, H. 1999. *The colloidal domain. Where physics, chemistry, biology and technology meet*, 2nd edition. Wiley-VCH, New York.

Everett, D. H. 1971. Manual of symbols and terminology for physicochemical quantities. Appendix II: Definitions, terminology and symbols in colloid and surface chemistry (Part 1). International Union of Pure and Applied Chemistry, Division of Physical Chemistry, Washington, D.C.

Glaus, M. A., Baeyens, B., Bradbury, M. H., Jakob, A., Van Loon, L. R. and Yaroshchuck, A. 2007. Diffusion of ^{22}Na and ^{85}Sr in montmorillonite: Evidence of interlayer diffusion being the dominant pathway at high compaction. *Environmental Science and Technology*, 41**,** 478-485.

Grim, R. E. 1968. *Clay mineralogy*. McGraw-Hill, New York.

Guldbrand, L., Jönsson, B., Wennerström, H. and Linse, P. 1984. Electrical double layer forces. A Monte Carlo study. *Journal of Chemical Physics*, 80, 2221-2227.

Hamaker, H. C. 1937. The London - van der Waals attraction between spherical particles. *Physica*, 4 (10), 1058-1072.

Helmy, A. K. 1998. The limited swelling of montmorillonite. *Journal of Colloid and Interface Science*, 207, 128-129.

Israelachvili, J. N. 1991. *Intermolecular and surface forces*. 2nd ed., Academic Press, New York.

Israelachvili, J. N. and Adams, G. E. 1978. Measurement of forces between two mica surfaces in aqueous electrolyte solutions in the range 0-100 nm. *Journal of the Chemical Society Faraday Transactions 1*, 74 (4), 975-1001.

Janiak, J., Jönsson, B., Jönsson, B. and Åkesson, T. 2008. Monte Carlo simulations of the swelling in bentonite clay. Presented at the Workshop on Buffer Erosion (V), January 28-29, 2008, Stockholm, Sweden.

Jansson, M. 2007. The DLVO theory. Presented at the Workshop on Buffer Erosion (III), March 29, 2007, Stockholm, Sweden.

Jansson, M. 2009. Laboratory studies of bentonite erosion. Report, Nuclear Chemistry, Royal Institute of Technology, KTH, Stockholm, Sweden.

Jönsson, B. and Wennerström, H. 1980. Ion condensation in lamellar liquid crystals. *Chemica Scripta*, 15, 40 -43.

Jusilla, P. 2007. Thermomechanics of swelling unsaturated porous media. STUK-A223, Radiation and Nuclear Safety Authority, Helsinki, Finland.

Khan, A., Jönsson, B. and Wennerström, H. 1985. Phase equilibria in the mixed sodium and calcium di-2-ethylhexylsulphosuccinate aqueous system. An illustration of repulsive and attractive double layer forces *Journal of Physical Chemistry*, 89, 5180 -5184 .

Karnland, O. 1997. Bentonite swelling pressure in strong NaCl solutions. SKB TR-97-31, Swedish Nuclear Fuel and Waste Management Co., Stockholm, Sweden.

Karnland, O., Muurinen, A. and Karlsson, F. 2002. Bentonite swelling pressure in NaCl solutions - experimentally determined data and model calculations. *In* Symposium on Large-Scale Field Tests in Granite, Sitges, Spain.

Karnland, O., Muurinen, A. and Karlsson, F. 2005. Bentonite swelling pressure in NaCl solutions – Experimentally determined data and model calculations. *In: Advances in Understanding Engineered Clay Barriers* (E. E. Alonso and A. Ledesma, eds.), Taylor & Francis Group, London, UK.

Kia, S. F., Fogler, H. S. and Reed, M. G. 1987. Effect of pH on colloidally induced fines migration. *Journal of Colloid and Interface Science*, 118 (1), 158-168.

Kjellander, R. and Marçelja, S. 1984. Correlation and image charge effects in electrical double layers. *Chemical Physics Letters*, 112, 49-53

Kjellander, R., Marčelja, S. and Quirk, J. P. 1988. Attractive double-layer interactions between calcium clay particles. *Journal of Colloid and Interface Science*, 126 (1), 194-211.

Kozaki, K., Fujishima, A., Sato, S. and Ohashi, H. 1998. Self-diffusion of sodium ions in compacted sodium montmorillonite. *Nuclear Technology*, 121**,** 63-69.

Kozaki, T., Inada, K. A., Sato, S. and Ohashi, H. 2001. Diffusion mechanism of chloride ions in sodium montmorillonite. *Journal of Contaminant Hydrology*, 47**,** 159-170.

Kozaki, T., Fujishima, A., Saito, N., Sato, S. and Ohashi, H. 2005. Effects of dry density and exchangeable cations on the diffusion process of sodium ions in compacted bentonite. *Engineering Geology*, 81**,** 246-254.

Kruyt, H. R. (ed.). 1952. *Colloid science*. Elsevier, New York.

Lagaly, G. 2006. Colloid clay science. In: *Handbook of clay science* (F. Bergaya, B. K. G. Theng and G. Lagaly, eds.). Developments in Clay Science, vol. 1, Elsevier Ltd., New York.

Langmuir, D. 1997. *Aqueous environmental geochemistry*. Prentice-Hall, Upper Saddle River, New Jersey.

Lifshitz, E. M. 1956. The theory of molecular attractive force between solids. *Soviet Physics*, 2 (1), 73.

Liu, J and Neretnieks, I. 2006. Physical and chemical stability of the bentonite buffer. SKB R-06-103, Swedish Nuclear Fuel and Waste Management Co., Stockholm, Sweden.

Liu, L., Moreno, L. and Neretnieks, I. 2009. A dynamic force balance model for colloidal expansion and its DLVO-based application. *Langmuir*, 25(2), 679-687.

Lyklema, J. 1991. *Fundamentals of interface and colloid science*. Vol. 1, Academic Press, London.

McBride, M. B. and Baveye, P. 2002. Diffuse double-layer models, long-range forces, and ordering in clay colloids. *Soil Science Society of America Journal*, 66, 1207-1217.

Miller, B. and Marcos, N. 2007. Process report - FEPs and scenarios for a spent fuel repository at Olkiluoto. Posiva 2007-12, Posiva Oy, Olkiluoto, Finland.

Missana, T. and Adell, A. 2000. On the applicability of DLVO theory to the prediction of clay colloids stability. *Journal of Colloid and Interface Science*, 230 (1), 150-156.

Missana, T., Alonso, U. and Turrero, M. J. 2003. Generation and stability of bentonite colloids at the bentonite/granite interface of a deep geological radioactive waste repository. *Journal of Contaminant Hydrol*ogy, 61, 17-31.

Moreno, L., Liu, L. and Neretnieks, I. 2008. Bentonite expansion into seeping water. Presented at the Workshop on Buffer Erosion (VI), December 9, 2008, Stockholm, Sweden.

Moreno, L., Liu, L. and Neretnieks, I. 2009. Modelling of erosion of bentonite gel by gel/sol flow. Report, Chemical Engineering and Technology, Royal Institute of Technology, Stockholm, Sweden.

Muurinen, A., and Carlsson, T. 2007. Development of methods for on-line measurements of chemical conditions in compacted bentonite. *Physics and Chemistry of the Earth*, 32**,** 241-246.

Neretnieks, I. 2009. Some scoping erosion experiments in thin slits between glass plates. Report, Chemical Engineering, Royal Institute of Technology, KTH, Stockholm, Sweden.

Neretnieks, I., Liu, L. and Moreno, L. 2009. Mechanisms and models for bentonite erosion. SKB TR-09-35, Swedish Nuclear Fuel and Waste Management Co., Stockholm, Sweden.

Pegado, L., Jönsson, B. and Wennerström, H. 2008. Ion-ion correlation attraction in a molecular solvent. *Journal of Chemical Physics*, 129 (18), 184503-1-9.

Posiva 2010. TKS-2009 nuclear waste management at the Olkiluoto and Loviisa power plants, review of current status and future plans for 2010-2012. Posiva Report TKS-2009, Posiva Oy, Eurajoki, Finland.

Puura, E. 2010. A review of natural cases and related laboratory experiments and the ideas on natural analogues for bentonite erosion/non-erosion. SKB TR-10-24. Swedish Nuclear Fuel and Waste Management Co., Stockholm, Sweden.

Richards, T. 2010. Particle clogging in porous media. SKB TR-10-22, Swedish Nuclear Fuel and Waste Management Co., Stockholm, Sweden.

Sato, T., Kuroda, M., Yokoyama, S., Tsutsui, M., Fukushi, K., Tanaka, T., and Nakayama, S. 2004. Dissolution mechanism and kinetics of smectite under alkaline conditions. *In* International Workshop on Bentonite-Cement Interaction in Repository Environments, Tokyo, Japan.

Savage, D., Arthur, R., Watson, C., and Wilson, J. 2010. An evaluation of models of bentonite pore water evolution. SSM Report 2010:12, Swedish Radiation Safety Authority, Stockholm, Sweden.

SKB 2004. Interim process report for the safety assessment SR-Can. SKB R 04-33, Swedish Nuclear Fuel and Waste Management Co., Stockholm, Sweden.

SKB. 2006a. Long-term safety for KBS-3 repositories at Forsmark and Laxemar – a first evaluation. SKB TR-06-09, Swedish Nuclear Fuel and Waste Management Co., Stockholm, Sweden.

SKB. 2006b. Buffer and backfill process report for the safety assessment SR-Can. SKB TR-06-18, Swedish Nuclear Fuel and Waste Management Co., Stockholm, Sweden.

Sposito, G. 1984. *The surface chemistry of soils*. Oxford University Press, New York, NY.

Stumm, W. and Morgan, J. J. 1996. *Aquatic chemistry, 3rd ed*. Wiley Interscience, John Wiley and Sons, New York.

Swanton, S. W. 1995. Modelling colloid transport in groundwater; The prediction of colloid stability and retention behaviour. *Advances in Colloid and Interface Science*, 54, 129-208.

van Olphen, J. H. 1977. *An introduction to clay colloid chemistry*, 2nd ed., Wiley-Interscience, New York.

Verwey, E. J. W. and Overbeek, J. T. G. 1948. *Theory of the stability of lyophobic colloids*. Elsevier, Amsterdam.

Wieland, E., Wanner, H., Albinsson, Y., Wersin, P. and Karnland, O. 1994. A surface chemical model of the bentonite-water interface and its implications for modelling the near field chemistry in a repository for spent fuel. SKB TR-94-26, Swedish Nuclear Fuel and Waste Management Co., Stockholm, Sweden.

2010:31

The Swedish Radiation Safety Authority has a comprehensive responsibility to ensure that society is safe from the effects of radiation. The Authority works to achieve radiation safety in a number of areas: nuclear power, medical care as well as commercial products and services. The Authority also works to achieve protection from natural radiation and to increase the level of radiation safety internationally.

The Swedish Radiation Safety Authority works proactively and preventively to protect people and the environment from the harmful effects of radiation, now and in the future. The Authority issues regulations and supervises compliance, while also supporting research, providing training and information, and issuing advice. Often, activities involving radiation require licences issued by the Authority. The Swedish Radiation Safety Authority maintains emergency preparedness around the clock with the aim of limiting the aftermath of radiation accidents and the unintentional spreading of radioactive substances. The Authority participates in international co-operation in order to promote radiation safety and finances projects aiming to raise the level of radiation safety in certain Eastern European countries.

The Authority reports to the Ministry of the Environment and has around 270 employees with competencies in the fields of engineering, natural and behavioural sciences, law, economics and communications. We have received quality, environmental and working environment certification.

Strålsäkerhetsmyndigheten
Swedish Radiation Safety Authority

SE-171 16 Stockholm
Solna strandväg 96

Tel: +46 8 799 40 00
Fax: +46 8 799 40 10

E-mail: registrator@ssm.se
Web: stralsakerhetsmyndigheten.se